Alma Mater Studiorum – Università di Bologna

DOTTORATO DI RICERCA IN

Biologia Molecolare e Cellulare

Ciclo XXXV

Settore Concorsuale: 5/E2 - BIOLOGIA MOLECOLARE

Settore Scientifico Disciplinare: BIO/11 – BIOLOGIA MOLECOLARE

TITOLO TESI

Design, expression, and characterization of FimH antigen as single recombinant protein or exposed on nanoparticles

Presentata da: Paolo Cinelli

Coordinatore Dottorato

Vincenzo Scarlato

Supervisore

Vincenzo Scarlato

Co-supervisore

Roberta Cozzi
Roberto Rosini

Esame finale anno 2023

1. **Introduction**
    - **1.1. *E. coli***
    - **1.2. Extraintestinal Pathogenic *E. coli (ExPEC)***
    - **1.3. Urinary tract infections (UTIs)**
    - **1.4. Pathogenicity**
    - **1.5. Pathogenesis**
    - **1.6. UPEC: the main cause of UTIs**
    - **1.7. Antibiotic resistance**
    - **1.8. Prophylactic and therapeutic strategies to tackle UPEC infections**
        - **1.8.1. Vaccines**
        - **1.8.2. Monoclonal antibodies: the case of mAb926**
    - **1.9. FimH, an attractive vaccine candidate**
    - **1.10. Nanoparticles as vaccine platform**
    - **1.11. Nanoparticle design**
    - **1.12. Engineering the external surface of NPs**
2. **Aim of the work**
3. **Materials and methods**
    - **3.1. Computational design and models prediction**
        - **3.1.1. Structure-based design of FimHDG and FimHDG-NPs**
        - **3.1.2. Model prediction using Rosetta Comparative Modelling**
    - **3.2. Cloning and expression in *E. coli***
    - **3.3. Expression in mammalian cell line**
    - **3.4. Monoclonal antibody production**
    - **3.5. Immobilized Metal Affinity Chromatography (IMAC)**
    - **3.6. Size Exclusion Chromatography (SEC)**
    - **3.7. Western Blot**
    - **3.8. SEC-HPLC and RP-UPLC**
    - **3.9. NanoDSF analysis**
    - **3.10. Surface plasmon resonance (SPR)**
    - **3.11. Transmission electron microscopy (TEM)**
    - **3.12. Immunization scheme**
    - **3.13. Enzyme-linked immunosorbent assay (ELISA)**
    - **3.14. Bacterial adhesion inhibition (BAI) assay**
4. **Results**

4.1. Computational structure-based design of stabilized monomeric FimH and FimH-stabilized nanoparticles
4.2. Stabilized FimH proteins and FimH-FimC complex are secreted and easily purified from a mammalian expression system
4.3. The C-terminal His-tag affects the folding of stabilized FimH antigen
4.4. Chimeric FimH_PGDGN_DG-Nanoparticles are secreted and correctly assembled when expressed in mammalian cells
4.5. FimHDG folding and stability is not affected by the display on nanoparticles
4.6. FimH stabilized with FimG donor strand is locked in the pre-binding conformation as demonstrated by the binding to mAb926
4.7. Recombinant FimHDG stabilized antigen and FimHDG-Ferritin are highly immunogenic in mouse
4.8. FimHDG and FimHDG-Ferritin candidates have a stronger capability to inhibit bacterial adhesion compared to FimHC benchmark
5. Conclusion and future perspectives

Abstract

Uropathogenic *Escherichia coli* (UPEC) accounts for approximately 85% of all urinary tract infections (UTIs), causing a severe global economic burden due to the hospitalization required to treat these infections and a decline in the quality of life for the affected subjects. Furthermore, *E. coli* is one of the pathogens mentioned in the ESKAPEE list drafted by OMS, meaning that the increasing antibiotic resistance acquired by this pathogen is and will be a serious health problem in the next future.

Amongst the immunogenic antigens exposed on the surface of uropathogenic *E. coli*, FimH represent a potential target for vaccine development, since it is involved in the early stages of infection, mediating the attachment of the bacterium to the surface of urothelial cells. As already demonstrated, immunizations with FimH elicit functional antibodies that prevent UPEC infections [1] even though the number of doses required to elicit a strong immune response is far from optimal.

In this work, we aimed to stabilize FimH as a soluble recombinant antigen exploiting the donor strand complementation mechanism by generating different chimeric constructs constituted by FimH and the donor strand of FimG. This approach allowed us to obtain a stabilized, soluble, and immunogenic version of FimH when expressed in mammalian cell lines.

The use of protein nanoparticles (NPs) as display platform has the potential to induce an enhanced immune response. To explore the potential of self-assembling nanoparticles to display FimH through genetic fusion, different constructs have been computationally designed and produced. In this work a structure-based design, using available crystal structures of FimH and three different NPs, *H. pylori* ferritin, encapsulin and mI3, was performed to generate different constructs with optimized structural and geometric properties.

Despite the different conditions tested, all the constructs designed (single antigen or chimeric NPs), resulted to be expressed as un-soluble proteins in E. coli. To overcome this issue a mammalian expression system has been tested to produce recombinant bacterial vaccine candidates. Soluble antigen expression was achieved for all constructs tested in the culture supernatants. Three novel chimeric NPs have been biochemically and structurally characterized by transmission electron microscopy (TEM) confirming the presence of correctly assembled NPs displaying UPEC antigen. In vivo study has shown a higher immunogenicity of the E. coli antigen when displayed on NPs surface compared to the single recombinant antigen. The antibodies elicited by chimeric NPs showed a higher functionality in the inhibition of bacterial adhesion.

1. Introduction

1.1. *E. coli*

Escherichia coli (*E. coli*) is a widespread facultative anaerobic, Gramm-negative, rod-shaped bacterium that colonizes the lower intestinal tract of warm-blooded animals, including humans [2]. While most of the *E. coli* strains are harmless commensals, some pathogenic variants can cause more or less severe infections in different tissues. Amongst all possible criteria that can be used to classify these bacteria the classical serological typing relies on O, H and K surface antigens. The O antigen is part of the *E. coli* lipopolysaccharide (LPS), which is composed by a core oligosaccharide with repeating O antigen subunits anchored on the surface of the bacterium by lipid A. So far, more than 180 different O antigens were described [3, 4]. K antigen is another polysaccharide antigen found on the surface of these bacteria and indicates the capsule that can or cannot be present depending on the strain considered. To date, more than 80 distinct types of K antigens are known [5]. Lastly, the H antigen identifies more than 50 different variants of flagellum [6, 7]. It is important to consider that each of these antigens can be found in any combination, leading to an enormous number of different strains differing in their immunological profile [8]. Other classification methods based on the phylogenetic analysis of *E. coli* population can be considered as described by Leimbach *et al.* [9].

E. coli pathotypes associated with intestinal diseases are generally classified as intestinal pathogenic *E. coli* (InPEC) or diarrheagenic *E. coli* (DEC), while those causing infections and diseases in other tissues are known collectively as extraintestinal pathogenic *E. coli* (ExPEC). *E. coli* that are pathogenic to the intestinal tract (InPEC) are obligate pathogens with distinct epidemiological and phylogenetic characteristics when compared with normal commensals or facultative ExPEC pathogens which belong to the normal gut flora where they live as commensals [10].

E. coli is a rapidly evolving bacterium. In addition to its conserved core of genes, necessary for important cellular processes, the E coli genome also contains a flexible gene pool which provides new pathogenic and metabolic traits, essential to adapt to constantly changing environmental conditions and to increase their fitness [11]. This flexible genomic portion is composed of accessory genetic elements like integrons, transposons, pathogenicity, and genomic islands (PAIs, GEIs respectively). In general, these islands are rarely fixed but are rather subject to ongoing rearrangement, deletions, and insertions; this phenomenon reflects also to the stable chromosomal

backbone that, together with the more plastic genomic portion, constantly undergoes repeated insertions and deletions. Therefore, homologous recombination of already existing gene blocks, together with the insertion of horizontally acquired DNA fragments make the *E. coli* genome rapidly and clonally evolving [12, 13].

This astonishing genomic plasticity, together with the ability to adapt to the most extreme conditions and pharmaceutical treatments, makes *E. coli* one of the main public health concerns, situation that is even more accentuated by the decline in antimicrobial drug discovery that characterizes this era [10]. Notably, outbreaks of new recombinant pathogenic *E. coli* were identified across the world as in the case of an enteroaggregative *E. coli* bearing several mobile genetic elements including the phage-mediated Shiga Toxin Stx2a and genes responsible for a broad antimicrobial resistance to, among others, third generation cephalosporins, trimethoprim/sulphonamide and tetracycline [14]. In addition to that, other studies report a correlation between foodborne *E. coli* and uropathogenic strains. This discovery changes the traditional foodborne illness paradigm, where the infection was located in the gastrointestinal tract upon ingestion of a sufficient dose of a pathogenic strain, and introduce the so called foodborne urinary tract infections (FUTIs) where the disease is caused by the ingestion of a uropathogenic strain of *E. coli* and, in a second step, its migration from the gastrointestinal tract to the urinary tract [15].

The involvement of uropathogenic isolates in foodborne disease and the appearance of new, virulent pathogenic *E. coli* strains, broadens and aggravates the implications of antibiotic resistance acquisition phenomenon.

In this context, given the alarming rate in antibiotic resistance cases, in 2017 the World Health Organization (WHO) communicated a prioritization list of pathogens (classified as critical, high, and medium priority) to guide the discovery of appropriate prophylactic and therapeutic strategies [16]. As part of the critical category of the WHO priority list, *E. coli* has become a healthcare concern due to the prominent level of resistance to many commercially available drugs [17]. It also represent one of the ESKAPEE (*Enterococcus faecium, Staphylococcus aureus, Klebsiella pneumoniae, Acinetobacter baumannii, Pseudomonas aeruginosa, Enterobacter spp.* and *Escherichia coli*) Gram-negative pathogens, so-called to emphasize their ability to evade the antibiotic activities leading to difficulties in treating such hospital infections [18].

1.2. Extraintestinal Pathogenic *E. coli (ExPEC)*

Given the nature and the diversity of this pathogen, ExPEC strains are able to invade and colonize many different tissues, causing infections and diseases in any age group, male or female. These pathogens are the most frequent causes of urinary tract infections (UTIs) and bacteremia, but they are also the pathogenic agent involved in infections of respiratory tract, skin, and soft tissues (figure 1) [8, 19]. The ability to colonize even the soft tissues leads to very severe and often life-threatening diseases such as neonatal meningitidis, pneumonia or peritonitis [20].

Given the high incidence of human infections globally [21-23] and the acquisition of antibiotic resistance plasmids such as extended spectrum β-lactamase and mobilized colistin resistance, these bacteria have been recognized as an important antimicrobial resistance (AMR) threats by the World Health Organization [24, 25].

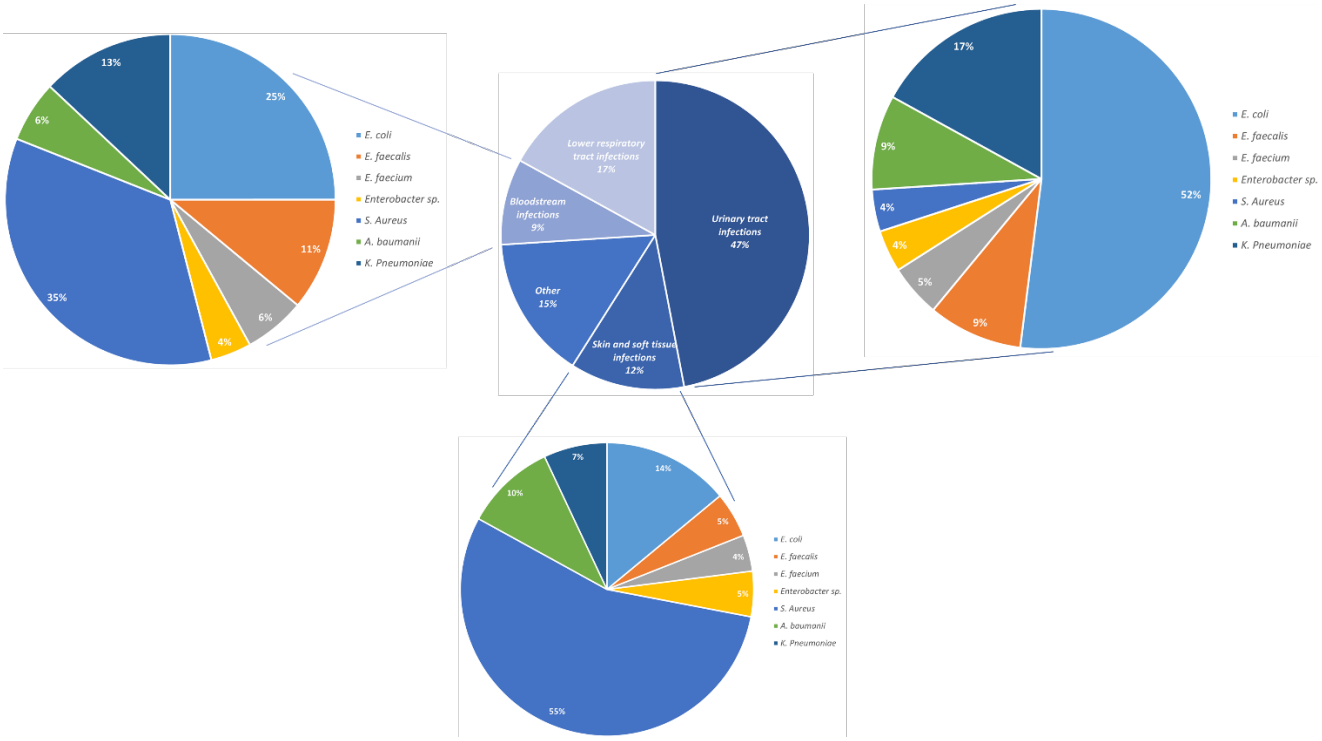

Figure 1. Pathogen distribution among isolates from over 80 thousand hospital admissions in US hospitals between 2007 and 2010. Abbreviations: E. coli: Escherichia coli; E. faecalis: Enterococcus faecalis; E. faecium: Enterococcus faecium; S. aureus: Staphylococcus aureus; A. baumannii: Acinetobacter baumannii; K. pneumoniae, Klebsiella pneumoniae.

As highlighted in figure 1, realized analysing samples form hospital admissions of more than 80 thousands subjects between 2007 and 2010 [26], *E. coli* accounts for more than 50% of urinary infections and, together with *Staphylococcus aureus*, is also the leading cause of bacteraemia

worldwide [27]. A large number of studies conducted across the world report that the overall incidence of annual cases of *E. coli* bacteraemia is strongly age-dependent, reaching more than 450 cases per 100 000 in individuals aged >85 years [27-29]. Similarly, the case-fatality rates for bacteraemia increase in elderly subjects, spanning from 13% in younger patients to up to 60% in elderly persons with already established nosocomial infections [29]. In light of these data and of the fact that the world elderly population continues to increase, with the number of individuals aged >65 years predicted to rise to 1 billion by 2030 and to 1.6 billion by 2050 [30], unless preventive action is taken, *E. coli* bacteraemia cases will increase accordingly. Another important aspect to consider is the source of bloodstream infections caused by *E. coli*. It is estimated, in fact, that more than 50% of *E. coli* bloodstream infections is originated by urinary tract infections making the urinary tract the most common source of bacteraemia [31].

For what it concerns the classification of the different ExPEC strains, two different definitions are commonly used. The first one relies on the number and diversity of virulence genes that they possess and is named "special pathogenicity" classification. In the "prevalence" definition instead, the distinction between the different strains is made taking into consideration the prevalence in the gut before they cause extraintestinal infections by mass action [32, 33]. Despite both classifications describe part of the complexity presented by the huge diversity of ExPEC strains, neither definition is truly adequate. In fact, even if many pathogenic *E. coli* lineages show overexpression of classic ExPEC virulence genes, the scientific community still struggles to distinguish between facultative ExPEC pathogens and commensal *E. coli* [34].

Amongst the extraintestinal pathogenic *E. coli* (ExPEC), four main pathovars were identified: uropathogenic *E. coli* (UPEC), neonatal meningitis *E. coli* (NMEC), septicemia-associated *E. coli* (SePEC) and avian pathogenic *E. coli* (APEC) [10].

1.3. Urinary tract infections (UTIs)

Urinary tract infections are characterized by an inflammation of the urothelium that occurs as a result of a microbial infection. In the first years of this millennium, urinary tract infections (UTIs) affected 150 million people yearly worldwide, resulting in at least USD 6 billion dollars (about USD 18 per person) of direct medical expenditures in the US only [35]. To have a better understanding of the impact that UTIs have on national health systems, it is useful to consider that nearly 8% of all hospitalizations and 0.9% of all outpatient and emergency room visits are caused by UTIs in the United States [36, 37]. Furthermore, there are 1.5 million UTIs associated with catheters implants

(catheter-associated UTIs or CAUTIs) in the United States every year, which is the second most common cause of healthcare-related infections, and 250 thousands cases of pyelonephritis yearly [22]. Considering other countries, the situation does not change. In England, for example, UTIs account for 17,2% of all nosocomial infections in hospitalized patients, making it the most common and widespread infection in these subjects [38]. Even if the real incidence of this pathology can only be inferred due to the different reporting methods and diagnostic criteria adopted across different countries, it is estimated that nearly half of the women will experience at least one UTIs in their lifetime, and half of these will also experience recurrencies within the following 6 month period [39, 40].

Taken together, these data show that UTIs are a significant source of morbidity and mortality worldwide, causing severe repercussions both on the affected subjects and the society [41]. The widespread nature of these infections, in fact, negatively affects not only the quality of life of the patients, that are often unable to perform their usual activities, but is also associated with a particularly high economic burden calculated in billions of dollars every year just in the US [42].

But why UTIs are so widespread across the world? One explanation can be found in the mechanisms of infection. The urinary tract, indeed, communicates with the outside and as a result, it is particularly susceptible to microbe invasion. Notably, some differences in the probability to develop a urinary tract infection exist between male and female subjects. The reason resides in the different anatomical conformation of the urinary tract, in women, in fact, the vaginal cavity and the rectal opening are closer to the urethral opening then in men. Furthermore, women present a moister periurethral area that favors bacterial growth and, as bacteria enter the urethra, they are more likely to reach the female bladder than the male bladder due to the shorter length of the urethra [43, 44].

Another reason why UTIs are becoming more and more frequent can be found in a study conducted in the USA between 2000 and 2009 that showed a 50% increase in hospitalizations caused by UTIs and a 300% increase of hospital admissions caused by extended-spectrum β-lactamase (ESBL)–producing *E. coli*, a pathogenic strain able to resist to first-line oral agents [37]. In fact, the dangerousness of these UPEC isolates resides also in their resistance to the most common broad-spectrum antibiotics like ampicillin, trimethoprim–sulfamethoxazole and fluoroquinolones as witnessed by recent antibiotic-resistant pathogenic *E. coli* outbreaks in the last years [45, 46].

Approximately, the 85% of all UTIs is caused by one main etiological agent: uropathogenic *Escherichia coli* (UPEC), which is able to colonize urinary tracts of sexually active women, neonates and elderly women and men [47, 48].

1.4. Pathogenicity

From a clinical perspective, UTIs are divided in uncomplicated and complicated. While uncomplicated UTIs typically occur in otherwise healthy individuals with no structural or neurological abnormalities in their urinary tract [49], there are a number of factors that contribute to complicated urinary tract infections, including obstruction, urinary retention caused by neurological diseases, transplantation, renal failure, immunosuppression, and foreign objects such as catheters, calculi, and other drainage devices [50, 51].

Furthermore, UTIs can be classified into lower UTIs, where the pathogen colonizes the lower urinary tract and determines the onset of cystitis, an upper UTIs, where the infection is spread to the upper part of the urinary tract and causes a pathology called pyelonephritis. In both cases, the incidence of these pathologies is an order of magnitude higher in women then in men, but this difference decrease with age [52-54].

UTIs have also the tendency to recur. Several studies conducted on different populations show that in subjects younger than 16 years of age, these infections have a probability of up to 22% to recur within 1 year and in sexually active women this probability increases up to 50% [55, 56]. Men are also susceptible to recurrencies, with an estimated probability of 8 to 12% to develop another UTI within 1 year [57]. The same reasoning also applies to the recurrence of pyelonephritis, the patterns by age and sex are indeed very similar with a higher prevalence in children under 16 years of age [43].

1.5. Pathogenesis

As the vast majority of UTIs are caused by uropathogenic bacteria that reside into the intestinal tract, in particular the uncomplicated ones, the first step to establish a urinary tract infection is the contamination of the periurethral area with a uropathogenic strain from the gut (step 1) as depicted in figure 2. Next, the pathogen colonizes the urethra and migrates to the bladder (step 2) where is able to adhere, colonize and invade the superficial umbrella cells, specialized cells that form the outermost layer of the urothelium, by expressing pili and adhesins [58]. In particular, UPEC can adhere to these cells thanks to the interaction between FimH, adhesion protein located at the tip of type I pili, and mannose fragments exposed on the surface of uroplakin Ia, a protein present on the surface of umbrella cell apical membrane that have the role to protect the mammalian bladder tissue from urine [59]. Complicated UTIs easily occur when a physical obstruction of the urinary tract is present, such as a catheter or kidney/bladder stones (figure 2, right) [60]. In these cases, it is very common to observe biofilm formation, an extracellular polymeric matrix that embeds microbial communities of

the surface-attached cells. The formation of biofilms decreases the susceptibility to antimicrobial agents enhancing the antimicrobial resistance phenomenon [61]. Once the colonization is established, the inflammatory responses begin to clear the pathogens from the bladder (step 4). However, in some cases we assist to the persistence of some bacteria that have the ability to evade the immune system going through morphological changes, that allow their escape from neutrophil killing, or by invading the host cells (step 5). These resistant pathogens can now replicate and form biofilms (step 6) [62]. In the meantime, the bacteria produce proteases and toxins that promote cell damage, this results in the release of nutrient and other element essential to the pathogens survival (step 7). From now on, bacteria can ascend the urinary tract (step 8) and establish a kidney colonization with severe consequences on the renal tissue (step 9 and 10). The close proximity and communication with the abdominal aorta and inferior vena cava make the kidneys a gateway to the bloodstream. If left untreated, in fact, uropathogenic bacteria can cross the tubular epithelial barrier in the kidneys and cause bacteraemia [63].

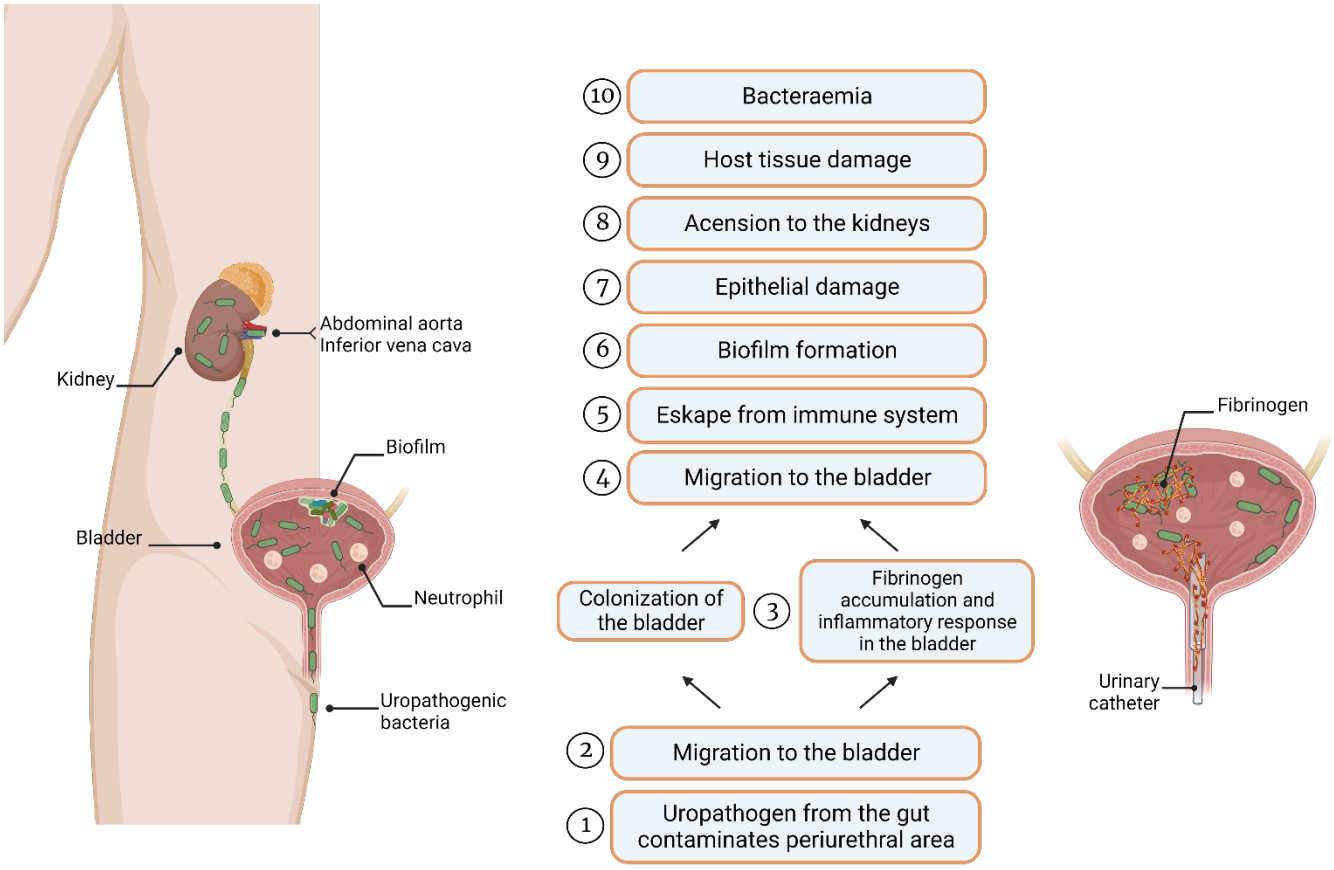

Figure 2. Pathogenesis of urinary tract infections. Schematic representation of lower and upper urinary tract infected and colonized by a uropathogenic strain. Uncomplicated UTIs are reported on the left while complicated UTIs caused by catheterization are reported on the right. Image adapted from [60] and realized with Biorender.

1.6. UPEC: the main cause of UTIs

Currently, uropathogenic *E. coli* strains are indistinguishable from strains that are responsible of extraintestinal infections. Among UPEC, five main phylogroups were identified: A, B1, B2, D and E relatively on their genetic relatedness [64]. This classification is based on the occurrence of genomic pathogenicity islands (PAIs), genetic elements on the chromosomes of many bacterial pathogens encoding virulence factors normally not present in non-pathogenic strains [65], and on the expression of several virulence factors, such as toxins, polysaccharides, adhesins and flagella [66].

In figure 3 are reported the main virulence factors presented by UPEC. Virtually all UPEC strains are surrounded by a polysaccharide coat, named capsule or K antigen, that is involved in the evasion form the immune system, preventing several killing mechanisms such as complement-mediated killing, opsonopahgocytosis and damage by antimicrobial peptides [5, 67]. Together with the capsule, UPEC present on its surface the lipopolysaccharide, named LPS, composed an oligosaccharide, the O antigen, anchored to the external membrane through lipid A. Analogously to the capsule, the LPS is able to "mask" subcapsular epitopes, preventing their recognition from host antibodies [68].

Moving form sugars to proteins, the first recognized virulence factors discovered in UPEC were adhesins, extracellular proteins involved in the attachment and invasion of host cells. Amongst all pilin and fimbrial adhesins encoded by UPEC, only a few of them, including P, Dr, and type 1 fimbriae, were considered for the development of a UTI vaccine. The P fimbriae, and in particular the protein located at the tip, PapG, is involved in the binding to Gal(α1-4) Gal-specific glycosphingolipids present in the kidney epithelium. Studies conducted using P fimbriae as vaccine candidate found it to be effective to prevent kidney infections [69, 70]. However, since this fimbria plays a role in the latter stages of the infection, a vaccine targeting P fimbriae will need to be combined with other component involved in the earlier stages of infections. Similarly to the P fimbriae, the Dr fimbriae is involved in the binding and colonization of the kidney since is able to bind the type 4 collagen present on the tubular basement membrane and Bowman's capsule [71]. Even in this case immunizations with Dr fimbriae were able to reduce the mortality associated to UPEC infections but didn't affect the rate of bladder or renal infection [72].

Differently to the previous fimbriae, the type 1 fimbria, and in particular the FimH, mediates the adherence to the bladder epithelium through the binding to mannose residues exposed on uroplakin, a structural component of this kind of epithelium [73]. Since this fimbria is involved in the early stages of the UPEC infection, a competitive inhibitor of FimH, such as methyl α-d-mannopyranoside [74], or a vaccine could potentially prevent the occurrence of cystitis. Supporting this thesis, a study

conducted on a knockout mutant UPEC strain lacking FimH revealed that this strain failed to bind human and mouse bladder epithelium but, by complementing it with a plasmid expressing FimH, the original phenotype could be restored [75]. Although several efforts to develop a type1 fimbria-based vaccine during the past years, to date an effective vaccine is still missing in the market.

Another kind of virulence factor presented by UPEC is the exotoxin. Vaccines based on toxoids, inactivated toxins, have been used against several bacterial pathogens and have been effective in preventing diseases such as tetanus, diphtheria and pertussis [76]. UPEC genome encodes for a plethora of exotoxins including CNF-1, cytolethal distending toxin, α-hemolysin and autotransporter toxins Pic, Sat and Tsh [77]. Even if many of these toxins have been associated with an increased symptom severity during UTIs, causing inflammation, epithelial disruption and renal damage, none of them have been shown to be necessary for the infection process, making these virulence factors not ideal for vaccine development [78, 79].

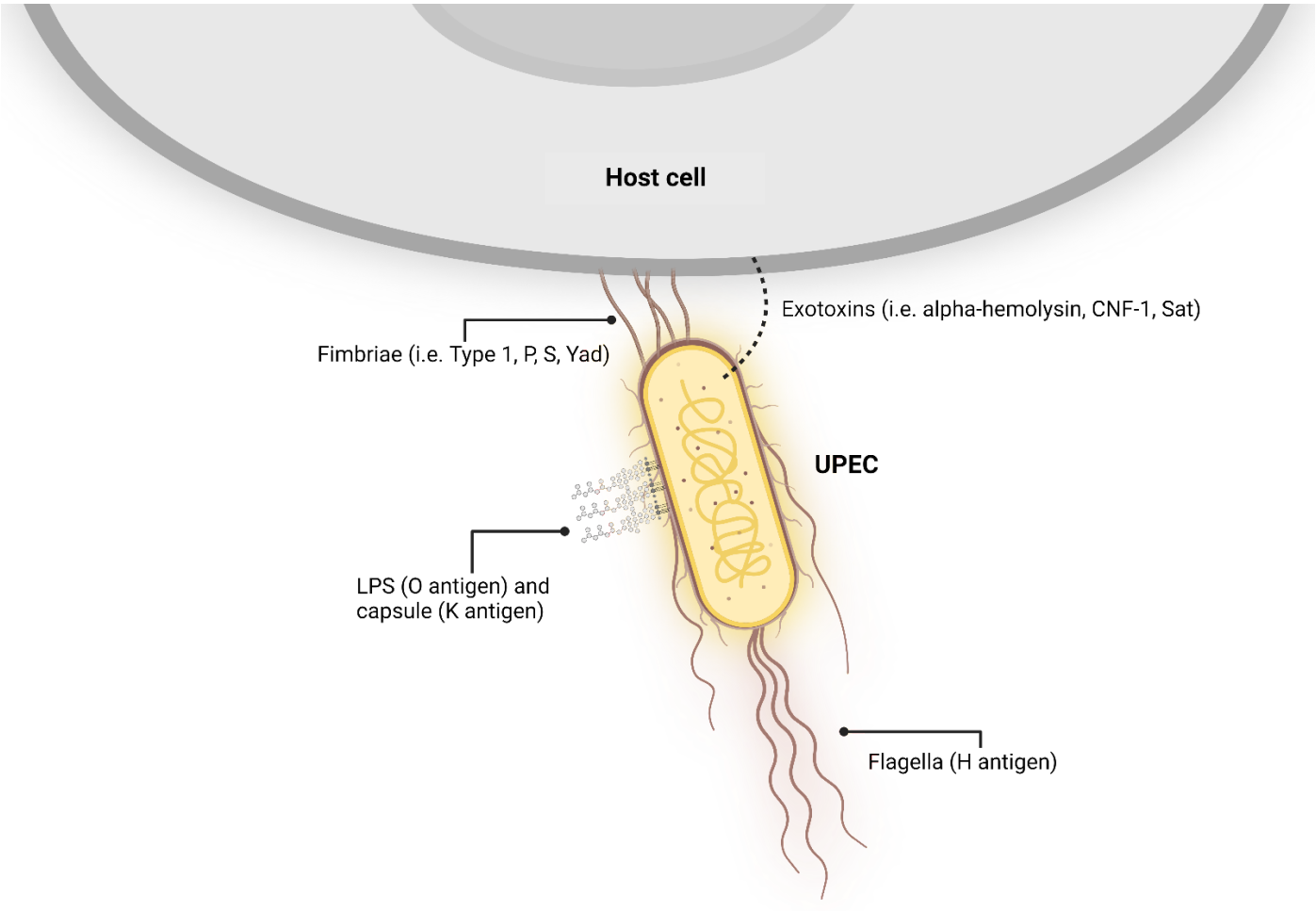

Figure 3. Schematic representation of the main virulence factors presented by UPEC.

As already mentioned, the vast majority of UTIs are caused by UPEC strains. Several studies conducted on different populations confirmed this trend. Among heathy young women between 18 and 39 years of age, *E. coli* is responsible to up to 80% of urinary tract infections [80]. *E. coli* was also found as the predominant cause of UTIs in hospitalized, ambulatory, and nursing home subjects with respectively a prevalence of 65%, 74% and 46% over all the other pathogens [39]. Among these, only *Staphylococcus saprophyticus* (1.4%), *Proteus mirabilis* (2.0%), *Streptococcus agalactiae* (2.8%), *Enterococcus* species (5.3*%)* and *Klebsiella pneumoniae* (6.2%) accounted for more than 1% of the remainder [81].

As *E. coli* is the leading cause of UTIs globally, we will focus on this pathogen to better understand how it spreads and how it can cause such a large number of infections.

The first step to get a better understanding of a pathogen is to understand how it is transmitted. Non uropathogenic *E. coli* and other *Enterobacteriaceae* colonize the gastrointestinal tract and if they make their way into the urinary tract they will be rapidly cleared. Instead, UPEC are highly adapted pathogenic bacteria able to initiate and maintain colonization in this environment, reason why they can reach more than 100.000cfu/mL in the urine [82]. As a consequence, it is very likely that they can spread from this environment pretty easily, for example they could contaminate the hands of an infected subject during urination. From there they can be then spread to other subjects through indirect transmission (contamination of water or food) or during a sexual intercourse. Indeed, sexual activity has been linked to UTIs as reported by several studies and by the fact that the incidence of UTIs is higher in women between 18 and 29 years, age when women are more likely to be sexually active [83, 84]. Another aspect linking sexual activity and UTIs onset is the fact that the same UPEC strain causing a UTI in a woman can be found with a high probability in the rectal or urethral districts of her most recent sexual partner [85].

In hospitalized patients, epidemics of nosocomial UTIs were also observed. In this case, the probability of developing a UTIs increases if the patient is catheterized or subjected to manipulation during surgery or medical care [86]. Most of these infections are therefore caused by two sources: the contaminated hands of hospital personnel that are in close contact with several patients, infected and not, and the bacteria already present in the perineal or rectal microbiota of catheterized subjects. In light of these mechanisms, it is of vital importance to adopt good hygiene practices and reduce or remove the catheters as quickly as possible to prevent the spread of bacteria causing catheter associated UTIs [87, 88].

1.7. Antibiotic resistance

Another aspect to take into consideration is the emergence of antibiotic resistant uropathogenic strains. As a consequence of prescribing antibiotics for treating UTIs without determining the bacteria involved, the number of uropathogens exposed to antibiotics increased, and the effectiveness of these oral therapies decreased [89]. To give an example of how widespread the antibiotic resistance is among these pathogens, in Europe the resistance to third generation cephalosporins and fluoroquinolones settles down to 11.8 and 22.3% respectively and in US, fluoroquinolone resistant UPEC are the 31% of the clinical isolates in hospitalized patients [26]. In other regions there is a considerable variation in the frequency of antibiotic resistant UPEC strains, for example, in Canada ampicillin resistant strains are the 33% of the total clinical isolates whereas in Mexico the frequency rises to almost 80% [90-92]. A similar trend was found for ciprofloxacin resistance, a common first line antibiotic used in uncomplicated UTIs. In this case the 72% of clinical isolates in Mexico was found resistant whereas a 10% was resistant in US and 0% in Canada [93].

In figure 4 is reported the chemical formula of the most representative antibiotics used to treat UTIs. In red are highlighted the antibiotics for which UPEC resistance has been demonstrated whereas in green are reported those antibiotics that still work to treat UTIs. Finally, in yellow are reported those antibiotics that are becoming ineffective for some cases of UTIs. In particular, among the most effective antibacterial compounds available, imipenem shows a 100% coverage on all UPEC strains followed by ertapenem, amikacin, and nitrofurantoin all above 99% of efficacy [94]. On the contrary, several UPEC strains show resistance to several traditional antibiotics such as ampicillin, trimethoprim-sulfamethoxazole, oral first-generation cephalosporins, cefuroxime, amoxicillin-clavulanate, cotrimoxazole, nalidixic acid, aminopenicillins and cefradine [95-98]. Finally, finafloxacin [99] and cefiderocol [100], two recently approved antibiotics in the US, showed promising results in threating multidrug-resistant UPEC strains.

Even if the situation is variable, the antibiotic resistance trend is worsening year by year and poses a serious global health problem. For this reason, in 2015 the European Association of Urology came out with new guidelines for the prevention of UTIs that were aimed to generate a behavioral change by each individual and adopt non-antibiotic measures for the first line treatment. If both of these strategies are not effective, then an antibiotic treatment is recommended considering the characteristics of the strain causing the infection [101].

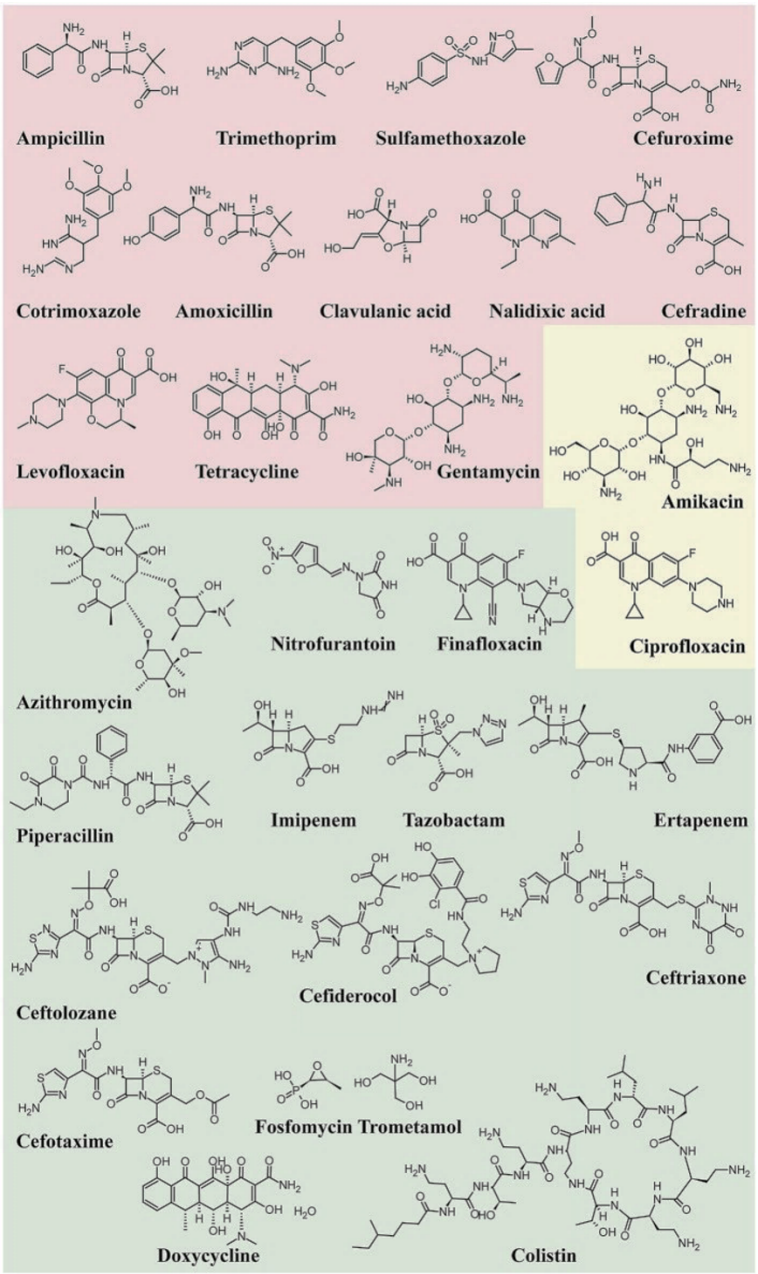

Figure 4. Structure of some antibiotics currently or previously used to treat urinary tract infections caused by UPEC. Red background: antibiotics against whom UPEC gained resistance; yellow background: antibiotics that show resistance in some, but not sill all, UPEC strains; green background: antibiotics effective against all known UPEC strains. Image adapted from [66].

Given the worldwide distribution of UPEC strain and their ability to acquire antibiotic resistance, the situation requires different strategies to address this emergency. One of the possible solutions could be the development of a vaccine against this pathogen.

1.8. Prophylactic and therapeutic strategies to tackle UPEC infections

As previously discussed, AMR has now become a public health concern, especially since many bacterial strains show resistance to a broad spectrum of antibiotics. In most cases, it is the result of pathogens evolving resistance through horizontal gene transfer and adapting to drugs due to their abuse, often deviating from the indicated dosage and inappropriate prescribing in medical practice. One further cause is the widespread and uncontrolled use of drugs in animals for increased meat production [102-106]. In this scenario, vaccines and monoclonal antibodies (mAbs) represent an important immunotherapeutic tool.

Indeed, the provision of an effective vaccine to protect populations has been recognized as an essential tool to fight AMR [107].

1.8.1. Vaccines

A major difficulty in producing a vaccine against ExPEC is the high similarity shared with commensal *E. coli* together with the broad variety of pathogenic *E. coli* strains that is circulating. Compared to drugs, vaccines have proven to provide a more sustained disease control being more robust against evolution of resistance. The main reason may reside in the prophylactic nature of the vaccines: while drugs are administered when a pathogen population is already large, vaccines are administered as soon as possible, lowering the possibilities for resistance to emerge [108] . In addition, the disease prevention made with vaccines decreases the need for antibiotic prescriptions and therefore the selective drug pressure that is responsible for the emergence of resistant strains [109-111]. Secondly, multivalent vaccines may induce immune responses against multiple targets on a pathogen, while drugs tend to target specific singular functions.

The development of vaccines to overcome the multidrug resistance problem has been unsuccessful so far due to the complexity and heterogeneity of ExPEC. Initially, several efforts have focused on vaccines to develop immunity against the polysaccharide antigens of different ExPEC serotypes, firstly using bivalent conjugate formulations and then with increasing valency [8, 112]. Currently, a plethora of vaccines is under development or already available to prevent UTIs and their recurrencies. They base their action on surface polysaccharides, surface antigens, i.e. hemolysins, iron acquisition systems, fimbrial adhesins and secreted proteins [113], or whole inactivated bacteria [114]. Uro-Vaxom, licensed in more than 30 countries, is an oral vaccine composed of crude extracts obtained

from 18 UPEC strains and several randomized placebo-controlled clinical trials have shown its efficacy to reduce the frequency of UTIs recurrencies

[115-119]. Another whole cell based vaccine is Urovac. This product is a multivalent vaginal vaccine made up of inactivated bacteria including six heat inactivated UPEC strains and other four uropathogenic strains.[120]. Even in this case, clinical trials demonstrated a reduction of UTI recurrencies during a 6-month period after immunization with this vaccine. [121]. Uromune is a sublingual vaccine composed of different inactivated uropathogenic strains, including *Klebsiella pneumoniae, Proteus vulgaris, Enterococcus faecalis and Escherichia coli,* currently pre-licensed in phase 3 stage. The efficacy of this vaccine was reported by prospective and retrospective uncontrolled studies showing a significant reduction of UTI recurrencies in women between 16 and 96 years old [122, 123]. However, given the 3-month daily administration period, the compliance of this treatment could be questioned considering. A FimCH-based vaccine is also under development against UTIs caused by *E. coli* and is moving to phase 2 clinical trials after successful phase 1 trials where it has proven to be immunogenic and safe [1]. Finally, ExPEC4V is the only vaccine exploiting the bioconjugation technique under prospective and retrospective uncontrolled studies. In this case, the O-antigens from four UPEC serotypes (O1A, O2, O6A and O25B), which are estimated to cover around 30-35% of all *E. coli* UTIs, were bioconjugated with *P. aeruginosa* exoprotein A as protein carrier [124]. This protein has been already used in the pseudomonal vaccine per se [125], but in the context of ExPEC4V, T-cell epitopes presented by exoprotein A were able to enhance the T-cell response against the bioconjugate LPS[124]. Data collected from three clinical trials showed that this vaccine candidate is well tolerated, meaning that it didn't raise any significant adverse effects, and immunogenic, since it was able to elicit a strong immune response towards all four serotypes for one year. On the counter side, ExPEC4V failed to reduce recurrencies. [126-128].

1.8.2. Monoclonal antibodies

Monoclonal antibodies, mAb, are designed and developed to specifically target and block a specific function of the protein of interest. Currently, only one mAb (A1124) is proposed to treat a colistin resistant ExPEC strain [129, 130]. This mAb targets the LPS O-antigen (O25b) of *E. coli* pointing out the importance of these kind of antigens to elicit a functional immune response [131].

Finally, previous studies have shown that antibodies raised against the type 1 pilus adhesion protein FimH, and in particular directed against its binding pocket epitopes, are neutralizing and highly efficient in preventing bacterial colonization [132-134].

Regarding FimH, a particularly interesting antibody was identified by Kisiela *et al* [135]. This mAb, named mAb926, is a parasteric antibody meaning that it binds to a portion of the binding pocket that does not directly compete with mannose for the binding to FimH, in contrast to mAb475, that directly competes with mannose for the binding [136]. Another interesting aspect of mAb926 is that it binds only to one specific conformation of the antigen, the low affinity one, meaning that is can also be used to screen the desired conformation of the antigen if used as a vaccine candidate.

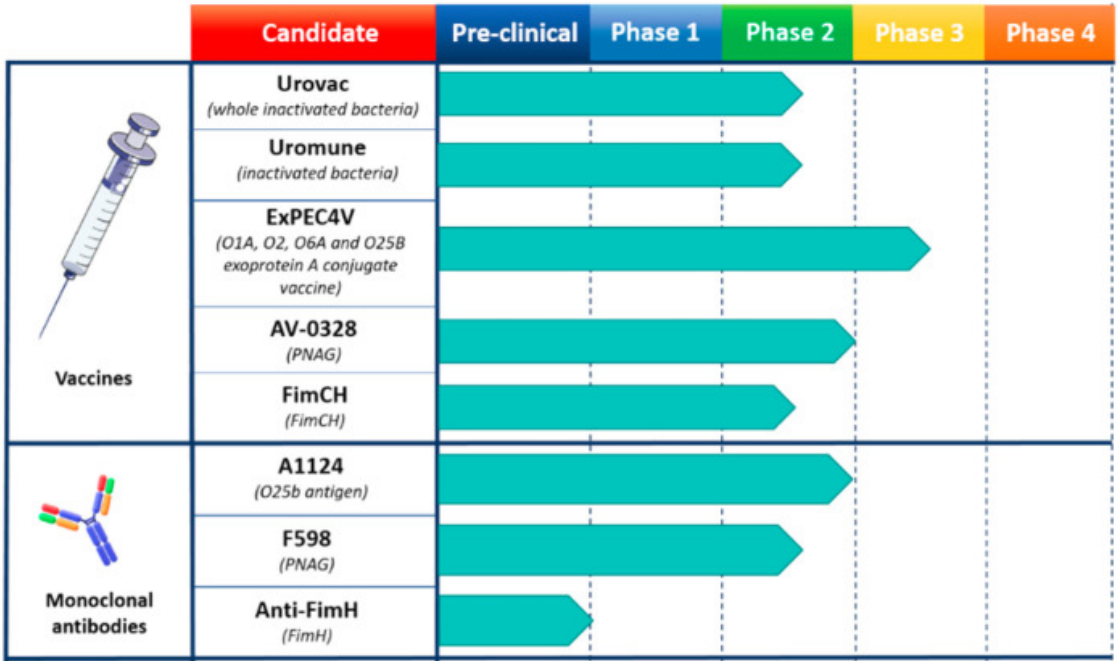

Figure 5. Human vaccines and monoclonal antibodies (mAbs) used to fight E. coli infections. The candidate section describes the trademarks and the specific targeted antigens. Pre-clinical as well as each clinical phase are represented. Arrows reaching dotted line indicate a completed study for that phase, conversely, studies are ongoing.

1.9. FimH, an attractive vaccine candidate

Bacterial adhesion plays a fundamental role in the establishment of a urinary infection. Indeed, the first step that allows UPEC to adhere and colonize the lower urinary tract is mediated by 0.1-2µm long, protein filaments located on the surface of these pathogens termed type 1 pili [137, 138]. Bladder invasion allows UPEC strains to replicate in a niche protected from innate immune defense mechanisms, antibiotics, and expulsion during urination [139]. A proof of the importance of this step is the fact that UPEC strains lacking type 1 pili are not able to invade the urothelium, thereby are rapidly cleared from the bladder without being able to cause any infection [140].

While the same cannot be said for other chaperone-usher pathway pili, such as the P pili, it is well documented that nearly all UPEC clinical isolates contain intact copies of type 1 pilus [141]. For this reason, type I pilus, and in particular FimH, the adhesin forming the tip, represent an interesting starting point for the development of an effective vaccine.

Type 1 pili are encoded by the *fim* operon, a contiguous DNA segment which encodes all the proteins necessary for their synthesis, assembly, and regulation. To date, nine genes have been identified and are reported in figure 6A [142]. These heteropolymeric type 1 pili are composed by a major pilus protein subunit (FimA) that builds the pilus rod, several minor adaptor proteins and chaperones (FimG, FimF, FimC, FimD) and a final adhesin at the distal end (FimH) that builds the distal tip [48, 143] (figure 6B). Among the elements that regulate the transcription of the *fim* operon we find *fimS,* located immediately upstream of the *fimA* gene [144]. *fimS* is a 314-bp invertible DNA element that contains the *fimA* promoter and undergoes a phenomenon called phase variation, where a 9bp long invertible element, labeled as IRR and IRL in figure 6A, is site-specifically recombined in either the Phase-OFF (nonpiliated phenotype) or Phase-ON (piliated phenotype) orientation [142, 144]. The main actors that regulate the phase variation phenomenon are two trans-acting factors encoded by *fimB* and *fimE* which are found upstream *fimS* [145]. These two elements can bind to the *fimS* sequence and drive the recombination to switch from Phase-ON to Phase-OFF or vice versa. It was found that *fimB* has a slight propensity towards the switch from Phase-OFF to Phase-ON, while the opposite transition is driven by *fimE* [146, 147].

While *fimI* function remains unclear [148], the function of FimC and FimD was well described. FimC is a periplasmic chaperon that binds the fim complex and helps the translocation to the outer membrane that happens thanks to FimD, an integral outer membrane protein that acts as an usher for the nascent pilus allowing its localization on the surface of the cell [149-151].

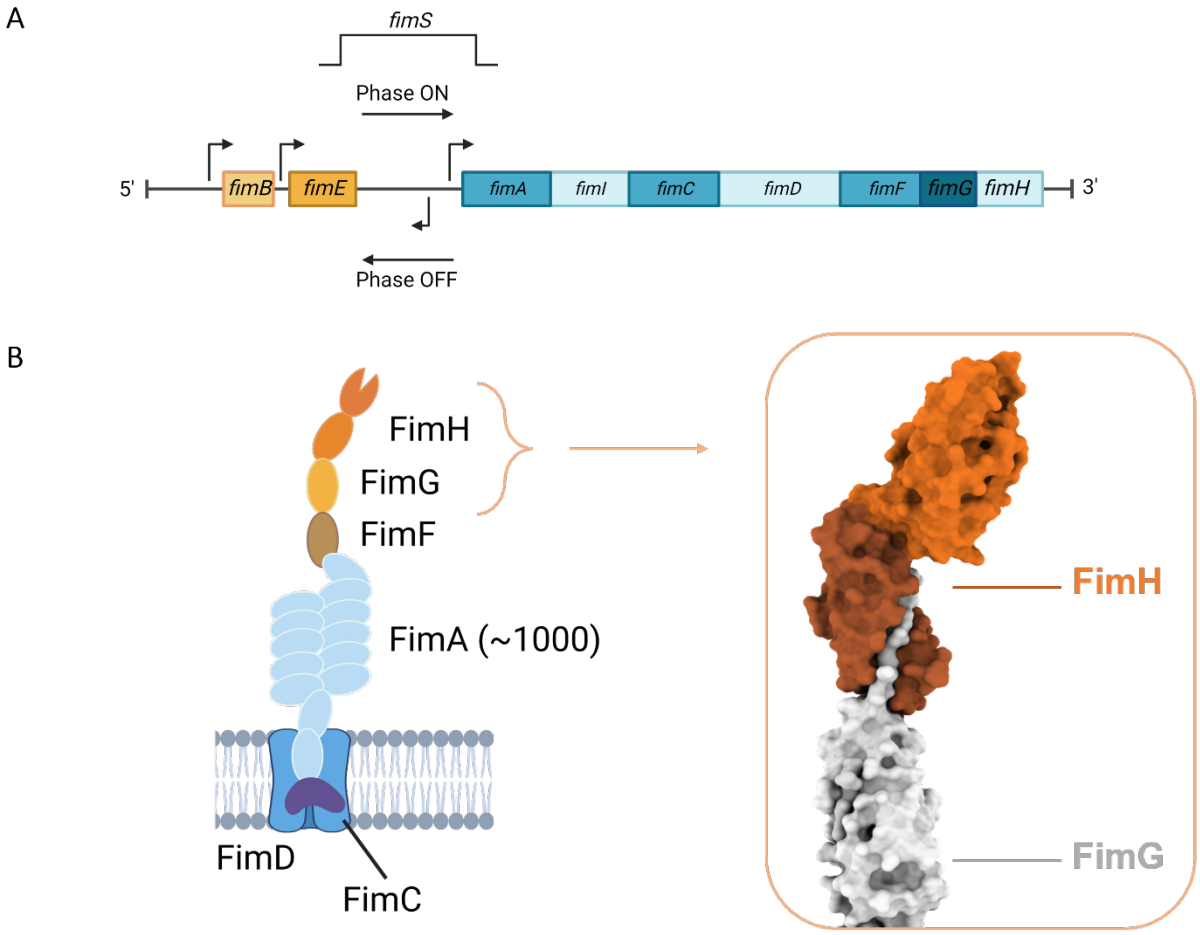

Figure 6. Top: Genetic organization of fim operon; bottom: type 1 pilus structure adapted from [152] and focus on FimH-FimG (right). Images were obtained using Biorender and UCSF ChimeraX software.

At the tip of the pilus we find FimH adhesin that specifically binds to terminal α-D-linked mannoses of N-linked glycans of uroplakin 1a located on urinary epithelial cells in a catch-bond mode [73, 153]. FimH is composed by two domains connected by a 5 amino acid linker (figure 7), the N-terminal domain is a mannoside-binding lectin domain (named FimHL) that can bind mannose residues through a pocket formed by three loops, whereas the C-terminal pilin domain (FimHP) is the one that attaches FimH to the pilus [154, 155]. This domain is folded into an immunoglobulin-like domain that is complemented by the donor strand from the chaperone FimC in the periplasm, and FimG when the pilus assembles [143]. This phenomenon is known as donor strand complementation and is necessary in order to stabilize FimH and to complete the pilus assembly connecting the tip to the rest of the assembled structure [156].

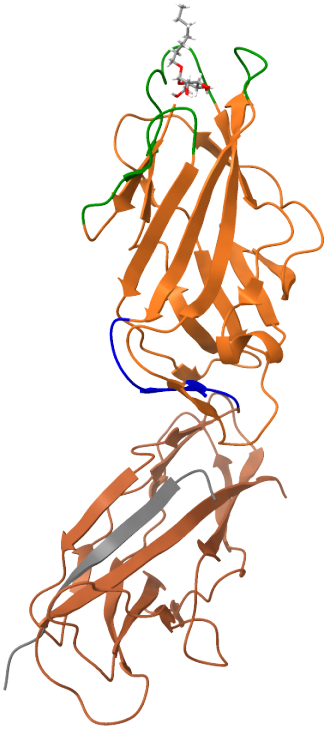

Figure 7. FimH structure representation adapted from 4XOB [157]. Pilin domain and lectin domain are represented in light and dark orange respectively. In the lectin domain the three loops responsible for mannose binding are highlighted (coloured in green): residues 8-16, 22-35 and 46-54. In licorice representation is reported the mannose. In blue is represented the linker loop that connects the two domains, residues 151-158. In the pilin domain the FimG donor strand is reported (in grey), that stabilizes the entire protein. Molecule visualization and representation was performed with UCSF ChimeraX software.

The two-domain architecture of FimH is functional for the catch-bond mechanism of the bacterial adhesin FimH to host epithelia. Indeed, the pilin and lectin domains interact with each other determining the conformational state and the binding properties of the lectin domain to the mannose ligand [153, 158] (figure 8). In particular, FimHP exist in only one conformation while FimHL can assume at least two major conformational states with different affinities for the ligand. In absence of ligand or other kinds of stimuli such as shear force, FimHL assumes a compressed conformation where the binding site is in an "open" state and interacts with FimHP via three loop segments: the linker (a.a 154-160), the swing (a.a. 27-33) and the insertion loop (a.a. 112-118) [156, 159]. In this case, FimHL is in a low-affinity mannose-binding state with an estimated K_D of 298 μM for the mannose. On the contrary, when the ligand or the periplasmic chaperon FimC are present and bound to FimH, FimHL assumes an extended conformation where the interactions between FimHL and FimHP are prevented [160-163]. A closed ligand-binding pocket and a rearranged swing, insertion loops and linker characterize the extended form of FimHL as well as a high affinity for the mannose, with an estimated K_D of 1,2 μM. Between these two opposite states, an intermediate conformation of

FimH characterized by a medium affinity for the mannose has been also reported. This intermediate conformation is transitory, meaning that there is an equilibrium between the low and medium affinity conformations in absence of stimuli.

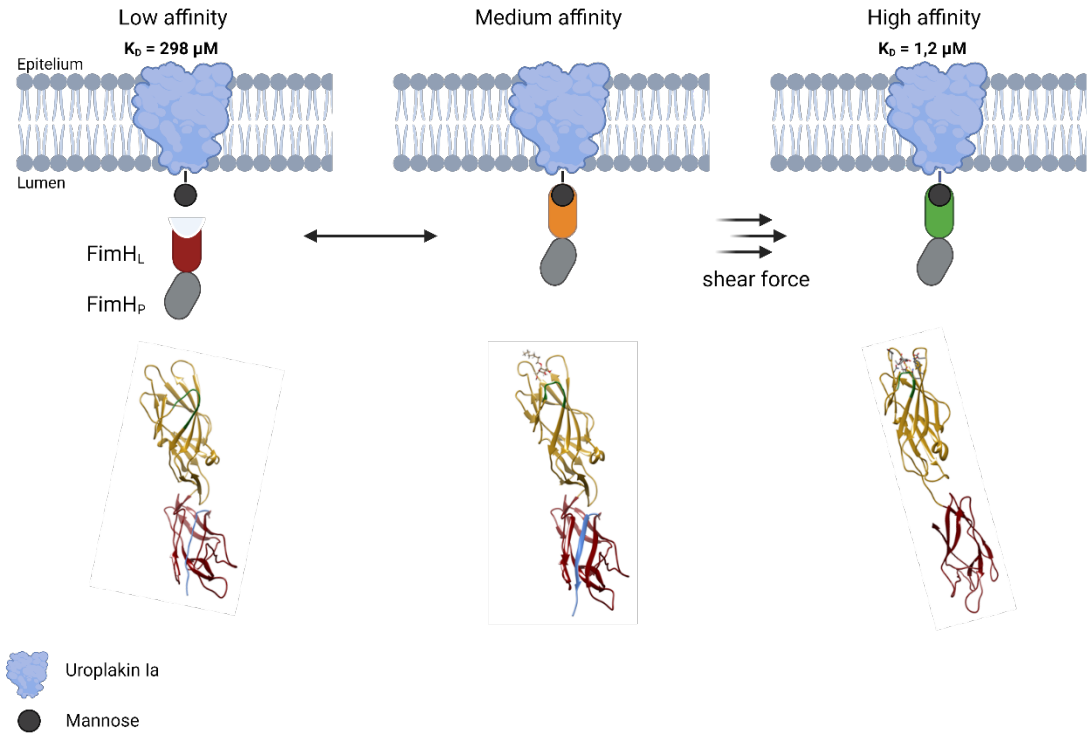

Figure 8. Schematic representation of FimH dynamic affinity to mannose in absence or presence of shear force. Mannose residues exposed on the surface of uroplakin Ia is boud by FimH with different affinities depending on the enviromental conditions. In absence of any stimuli, FimH oscillates between a low and medium mannose affinity confomation whereas, upon shear force application, FimH assumes a high mannose affinity conformation. Image realised using Biorender.

Among the stimuli that can trigger mannose binding, the shear force acts as a mechanical allosteric effector allowing the catch-bond mechanism and consequently the adhesion of bacteria to the surface of the urothelium [164, 165]. This mechanism is particularly useful since it allows the bacteria to attach and to be retained in the bladder, avoiding the elimination by micturition [142].

FimH is a phase variable protein, and its expression is regulated by environmental signals within the urinary tract (salt, growth conditions and acidic pH). Due to its crucial role in the *E. coli* pathogenicity several attempts were made to identify competitive inhibitor of FimH binding [166, 167] as possible drugs or to develop vaccines based on FimH as main antigen [168, 169]. Recently, a recombinant based vaccine against UTIs produced by Sequoia Sciences started the Phase 2 of clinical trial. FimH

recombinant antigen formulated with an adjuvant in phase-1 clinical trial could reduce the frequency of UTI in adult women with 2 years of previous infections [1, 170]. However, this vaccine preparation, based on the recombinant adjuvanted complex FimH-FimC needed the administration of 4 doses to elicit a sustained immune response, leaving room for the development of an improved FimH-based vaccine.

1.10. Nanoparticles as vaccine platform

During the years, vaccine development led to increasingly sophisticated and tailored vaccines, able to elicit strong immune response against the pathogen of interest. The first examples of vaccines were the one produced attenuating the pathogen through the application of a selective pressure, making the pathogen less virulent and harmless to the subjects receiving the vaccine [171]. This kind of vaccines are able to elicit a very strong and long-lasting immune response but they also rise some safety concerns due to their potential to revert into pathogenic viruses [172]. Similar to the attenuated vaccines, inactivated or killed vaccines exploit the entire pathogen to elicit an immune response. In this case the pathogen is treated and killed by using heat, chemicals, or radiations [173]. During the years several inactivated vaccines were developed against a wide variety of pathogens such as: typhoid [174], cholera [175, 176], pertussis [177] and influenza [178] among others. While these inactivated pathogens cannot replicate or revert into virulent forms that make them safer compared to the attenuated ones, they tend to stimulate a weaker immune response, leading to the need of multiple immunizations and adjuvants to stimulate the immune system [179].

To address these limitations, self-assembling proteins which can fold into geometrically defined 3D structures, such as nanoparticles (NPs), can be used to mediate multicopy antigen display. Indeed, from some years now, self-assembling protein nanoparticles and virus like particles (VLPs) are widely used in vaccinology as a platform for antigen presentation to increase the immunogenicity of recombinant-based vaccines [180]. In fact, the multicopy display of a target antigen on a larger scaffold improves the APC uptake and the retention in follicles with the potential to induce potent B- and T-cell responses [181]. During the years, several different NP-based vaccines have been licensed against different viral pathogens such as *papilloma virus*, *hepatitis B,* and *hepatitis E* viruses [182-185]. Currently chimeric NPs displaying also bacterial antigens have been investigated in preclinical studies worldwide [186] as well as against malaria [187, 188]. In particular, it has been shown that chimeric AP205 displaying enterotoxigenic *E. coli* antigen was able to elicit neutralizing antibodies in mice [189].

1.11. Nanoparticle design

An important aspect to consider when working with self-assembling protein nanoparticles is the feasibility to engineer them by fusing or linking the antigen of interest. In these last twenty years, a lot of progresses were made in the field of structural biology, and these achievements led to the possibility to rationally design new vaccines on the basis of the structure of both antigen and newly designed carriers [190]. The structure-based design has also seen important advancements with the appearance of computational approaches able to direct the design of nanoparticle carriers. To date, three main approaches for the design and engineering of protein nanoparticles have been explored: modification of existing natural NPs (top-down approach), *de novo* design of new NPs (bottom-up approach), and evolution of natural NPs to confer specific functions to the carrier [191]. The top-down approach is the most straightforward since the NPs used are already present in nature and are modified to display on their surface antigens of interest, in case of vaccine application [192]. The NPs used are extremely optimized proteins that evolved during millions of years to specialize in some precise functions, such as in the case of ferritins, encapsulins, and lumazine synthases and gained characteristics difficult to recreate using current design methods [193-195]. A drawback of this approach is that the design space is limited to the characteristics of the carrier, limiting the possibilities to create new chimeric NPs. On the other side, the bottom-up approach enables the design of *de novo* designed peptides able to self-assemble into the desired 3D conformation, expanding the breath of possible innovative designs [196-198]. This approach has seen a rapid development thanks to new computational methods that allowed protein interface and rigid body designs as reported by King et al. [199]. Even if the traditional method for computational design requires highly specialized knowledge and high computational resources, new advances in machine learning are rapidly revolutionizing the design process, simplifying the workflow, and minimizing the computational cost thus making the computational design a more accessible technique [200].

1.12. Engineering the external surface of NPs

To modify the exterior surfaces of NPs with the intent to display to the immune system the antigen of interest, three main strategies can be adopted. The most straightforward approach is the genetic fusion. Here, upon a structural evaluation of both carrier and antigen, the two “building blocks” are joined together by an aminoacidic linker. The designed chimeric DNA sequence is translated into the corresponding chimeric protein using the preferred expression system, bacterial or mammalian, and purified using different methods based on chemical or/and physical properties. The strength of this

approach relies in the homogeneity of the product, since the chimeric proteins are genetically encoded, and in the simplicity of the production process, which requires very few steps to obtain a purified final product. An alternative approach is the chemical conjugation. In this case antigen and carrier are joined together exploiting a chemical reaction between reactive groups such as lysine or cysteine residues [201]. In this case, the production of decorated NPs requires several steps of production and purification since the two components must be expressed and purified separately, mixed, and re-purified to discard all the unbound. All these steps require longer timelines at the same time lowering the yield of conjugated NPs [202, 203]. Lastly, the protein ligation phenomenon can be exploited to decorate the surface of NPs. In this case, two peptides covalently interact to form an irreversible intermolecular isopeptide bond. Using this approach can alleviate the problems regarding protein folding, suboptimal expression host or post-translational modifications by separating the production of the proteins. During the years several system have been designed, including SpyTag/SpyCatcher [204, 205], split intein [206] and SortaseA [207, 208].

2. Aim of the work

The focus of this work was to design and develop a vaccine candidate based on FimH antigen with the final objective to advance the discovery of a vaccine against ExPEC, which cause the vast majority of UTIs.

Previous attempts to develop a FimH-based vaccine were made but, since its low immunogenicity in human, the available vaccine candidates required at least four doses to elicit 150-fold increases in antibodies against the N-terminal region of FimH. This limitation leaves space for further optimization and, since the nanoparticle technology is rising as a new and powerful vaccine platform, we reasoned that FimH immunogenicity could increase if exposed on the surface of a NP.

Since FimH is able to elicit more potent neutralizing and functional antibodies when presented in the low-mannose binding affinity conformation, the first goal was to design a stabilized version of FimH in this specific conformation. To this aim, the donor strand of FimG was genetically fused to the antigen through a semi-rigid linker. This stabilized FimH, called FimHDG has been further compared to FimHL_Cys, a FimHL domain stabilized by an internal additional disulphide bond, in a low affinity conformation. The successive objective was then to decorate three different NPs as antigen carriers with the stabilized FimH. Ferritin, mI3 and encapsulin are the NPs selected for this study.

3. Materials and methods

3.1. Computational design and models prediction

3.1.1. Structure-based design of FimHDG and FimHDG-NPs

Crystal structure of *E. coli* type I pilus was downloaded from the Protein Data Bank with PDB code 3JWN. This PDB includes the crystal structures of FimC, FimF, FimG and FimH in complex to form an incomplete pilus. The crystal was visualised using Pymol software and the FimH structure was isolated from the complex together with the donor strand from FimG. From this starting structure, a structure-based approach was adopted to design a stabilized, un-complexed full-length FimH where the donor strand peptide from FimG was genetically fused through a linker of 4 or 5 amino acids, DNKQ and PGDGN respectively. The linkers were manually constructed by adding one residue at a time in order to satisfy the following criteria: occupancy of allowed zones of Ramachandran plot to obtain the correct secondary structure, absence of any steric hindrance following the insertion of each residue, and maximization of stabilizing interaction between the side chains of the linker and the local structure to lock the prebinding conformation of FimH. To ensure that each residue of the linker did not clash with the secondary structure of FimH, each aminoacidic insertion was followed by the check of steric hindrance by calculating the Van der Waals radii with Swiss-PdbViewer [209]. Once the linker construction was done, the structure was minimized using the Swiss-PdbViewer built-in GROMOS96 force field until the delta free energy between two steps was below 0,05 KJ/mol.

3.1.2. Model prediction using Rosetta Comparative Modelling

The 3D structure predictions of each chimeric nanoparticle displaying FimHDG were obtained with Rosetta comparative modelling tool [210]. To obtain the antigen-decorated scaffold, a model composed of the nanoparticle monomer and FimHDG was manually prepared and aligned to the asymmetric unit of the self-assembling particle [211]. Then, a linker connecting the two portions was conformationally sampled using a fragment-based loop-modelling protocol, with refinement in Rosetta to minimize energetics and resolve clashes [212]. Finally, symmetric constraints were applied to generate the other subunits to obtain a 3D structure prediction of the entire nanoparticle. Pymol [213] and ChimeraX [214] software packages were used for structural investigation, molecule visualization and graphical representation.

3.2. Cloning and expression in *E. coli*

FimH-NPs bacterial constructs were synthetized as DNA strings by GeneArt (Thermofisher) and then cloned into pET21b+, pET22b+ and pET15b+ commercial plasmids (Merck-Sigma) to obtain recombinant N- or C- terminally His-tagged proteins, using the Takara infusion cloning kit following manufacturer instructions. Optimization of the codon usage for expression in the E. coli, along with the addition at the gene extremities of the appropriate linker for ligation independent cloning were performed. Insertion of His Tag facilitates the purification process by immobilized metal affinity chromatography (IMAC).

After cloning, the correct sequence of selected clones was confirmed by NGS sequencing.

Protein expression was performed using E. coli BL21(DE3) strain (New England Biolabs) and T7shuffle Express (New England Biolabs). The cells were grown in 10 mL of HTMC media (Glycerol 15 g/L; Yeast Extract 30 g/L; MgSO4 x7H2O 0.5 g/L; KH2PO4 5 g/L; K2HPO4 20 g/L; KOH 1 M to pH final 7.35±0.1), under shaking (160 rpm) at 37° for 12 hours and then diluted 1:100 in a final volume of 75 mL of HTMC. Bacterial cultures were then incubated at 20°C under shaking conditions overnight, followed by the induction with 1mM IPTG for 24 hours at 20°C at 160 rpm. All the liquid cultures were pelleted (15 minutes, 3000xg) and resuspended in cell lytic express (Merk) or B-Per (Pierce) lysis buffer for 1 hour at 25°C. To allow the separation of the insoluble fraction from the soluble one, a 30-minute centrifugation at 15000xg was applied. After this step, a pellet corresponding to inclusion bodies (IB) was visible. To resuspend the precipitated proteins, 8M Urea was used as denaturating agent. The presence of chimeric proteins was assessed by SDS-Page analysis loading the soluble (S) and denaturated insoluble fraction (IB).

FimHC complex was expressed using a plasmid with a dicistronic operon under control of the trc promoter in the periplasm of *E. coli* BL21(DE3) as already described by Glockshuber *et al* [215].

3.3. Expression in mammalian cell line

FimH-NPs constructs for mammalian expression were synthetized as DNA synthetic genes already cloned into pCDNA3.1or pCDNA3.4 vectors by GeneArt. All constructs were codon optimized for mammalian expression and all contain an N-terminal leader sequence for secretion into the medium.

Two modified versions of the IgK murine leader sequence were tested in this study. The cell lines used to express the chimeras were the Expi293, ExpiCHO and Expi293GnTI cells (Lifetechnologies).

Expi293GnTI cell line derives from the Expi293F but lacks the N-acetylglucosaminyltransferase I (GnTI), responsible for the transfer of a GlcNAc residue from UDP-GlcNAc to the acceptor substrate Man5GlcNAc2 to produce GlcNAcMan5GlcNAc2, needed for the action of all subsequent processing enzymes. Therefore, the lack of GnTI prevent the N-glycosylation with complex glycans, leading to more homogeneously glycosylated recombinant proteins.

For the transfection, we followed the manufacturer protocol; briefly, 30 mL culture containing 3-4 x 10^6 mammalian cells were transfected with 30µg of pCDNA vector encoding for FimH-NPs using ExpiFectamine 293 reagent. Cells were then incubated at 37°C, with 8% CO_2 at 120 rpm. After 24 hours, ExpiFectamine transfection enhancers 1 and 2 were added accordingly to the culture volume. Cells were then incubated at the same conditions for 5-6 days. Every 24 hours, aliquots of cultures were harvested to monitor protein expression by sodium dodecyl sulphate-poly-acrylamide (SDS-PAGE) and Western Blot analysis. The sixth day, cultures were pelleted (7 minutes, 1000 rpm) and the clarified supernatant was filtered with 0,22µm filers. All the filtered supernatants were immediately processed or stored at -20°C until purification.

3.4. Monoclonal antibody production

The monoclonal antibody selected to screen the different conformation of FimH constructs was mA926 since it is a conformational antibody binding the pre-binding conformation of FimH as already reported by Kisiela *et al* [135]. The antibody expression and purification were externalized to Thermofisher Scientific GeneArt using the sequence reported in literature.

3.5. Immobilized Metal Affinity Chromatography (IMAC)

The first protein purification step was performed by immobilized metal affinity chromatography (IMAC) using Ni-NTA agarose resin (Thermo Fisher Scientific), a wash buffer containing PBS and 20 mM of imidazole and an elution buffer containing phosphate buffered saline (PBS) with 350mM of imidazole. Briefly, the unpurified sample was loaded into a column previously packed with Ni-NTA agarose resin. The sample was incubated at room temperature for 5 minutes and afterwards the flowthrough was collected in an empty falcon. The resin was then washed with 10 column volumes using PBS + 20 mM imidazole to detach any unspecific protein but not the protein of interest. The elution step was performed with PBS + 350 mM imidazole and the chimeric protein was recovered in an empty falcon.

For those constructs lacking the His-Tag, the first purification step consisted in a size-dependent concentration using 300 kDa cut-off spin concentrator (Amicon Ultra Centrifugal Filters) following by 5 washing steps with PBS to further remove small size protein contaminants.

3.6. Size Exclusion Chromatography (SEC)

Fractions containing the target protein were pooled, concentrated and loaded into a size exclusion chromatography (SEC) column (Superdex 200 10/300 or HiLoad 26/600 superdex 200, Cytiva) equilibrated in PBS buffer, with a flow rate of 0.5 mL/min or 2ml\min depending on the column size volume. Due to their large sizes the NP proteins were collected in the void volume. SDS-PAGE and western blot analysis were performed to check protein purity and the concentration was determined by UV-Vis absorbance at 280nm (Nanodrop device) on the final pooled fractions.

3.7. Western Blot

1 µg of purified proteins were loaded on a 4 to 12% Bis-Tris NuPAGE gel (LifeTecnologies) and run for 30 minutes at 180 V. The proteins were then transferred to a nitrocellulose membrane using the iBlot gel transfer device (Thermofisher) using the manufacturer protocol. Upon proteins transferring, the membrane colored by ponceau reagent to confirm protein transferring, washed 3 times with PBS and blocked with 3% milk in PBS and 0.1% Tween detergent. The binding with primary antibody (in 3% milk) was done for 1h at room temperature (18-26°C) with gentle shaking, then the membrane was washed three times with 10mL of PBS and 0.1% Tween for 5 minutes each. The secondary antibody conjugated with horseradish peroxidase (HRP) was added (diluted 1:1000) in 3% milk to the membrane for 1h. Three additional washing steps were performed, as above, before adding the chromogenic substrate 4-chloro-1-naphthol to acquire the signal using GelDoc XR+ imaging system. The primary antibodies used were the anti-his-HRP conjugated antibodies by Sigma (diluted 1:1000) or the anti FimHL-cys antibodies (diluted 1:1000) raised in mice using the FimHL-cys recombinant pure protein. In the latter case, a secondary HRP-conjugated anti-mouse antibody was used (diluted 1:1000) to detect the signal.

3.8. SEC-HPLC and RP-UPLC

To assess protein size and purity, analytical SEC-HPLC and reverse phase RP-UPLC were performed. For the SEC-HPLC, the following protocol was adopted: about 5µg of sample were loaded into SRT-C 2000 column using NaPi 100mM pH 7,2 + Na2SO4 100mM as running buffer. The flow was set at 0,4 ml/min. The absorbance at 214 nm, 280 nm e 254 nm were constantly measured. Elution fractions containing molecule of interest were collected, pooled, and stored at 4°C.

The RP-UPLC was performed adopting the following protocol: 50 µl of previously purified protein sample were loaded into a Acquity UPLC Protein BEH C4 2,1x150 mm. The mobile phase buffer (buffer A) was composed by 0,1% trifluoroacetic acid (TFA) in water while the second buffer (buffer B) was composed of and 0.1% TFA in acetonitrile (ACN). The flow was set at 0,4 ml/min. Below in the table are reported the concentration variations of A and B buffer during time

Time	%A	%B
0	100	0
2,5	100	0
13	0	100
13,2	0	100
13,3	100	0
15	100	0

Absorbance at 215 nm and 280 nm was constantly measured.

3.9. NanoDSF analysis

To assess the stability of each construct, a nano-DSF analysis was performed. This technique monitors the fluorescence caused by the unfolding of the protein, hence the exposure of hydrophobic residues. Samples were manually loaded into nano-DSF grade standard capillaries and transferred to the nano-DSF device (Prometheus NT.48). In order to measure the fluorescence of the exposed tryptophan residues, samples were excited with a 280nm wavelength, and the readouts were conducted at 330nm, 350nm and 350/330 nm ratio. Analysis of data was conducted using Prometheus PR. Control software from NanoTemper Technologies.

3.10. Surface plasmon resonance (SPR)

To study the molecular interaction between FimHDG constructs and mAb926 or mAb475, two murine monoclonal antibodies known to bind the antigen in two different sites [135], and between FimHDG and mannose, SPR analysis were conducted.

FimHDG constructs were diluted with running buffer composed by HBS-EP + 0,01M HEPES, 0,003M EDTA, 0,15M NaCl and 0,05% v/v Surfactant P20. A sensor chip NTA (Cytiva) was activated by injecting a solution of Ni^{2+} 0,5mM and then washing three times with 3mM of EDTA. The prepared samples were then captured on the surface of the activated chip. Similarly, the mAbs were captured on the surface of a CM5 sensor coated with secondary anti-mouse IgG Fc using a concentration of 20µg/ml. 50 mM of each sample was injected on the surface of the sensor chip for 180 seconds. The dissociation profile was followed for 600 seconds and following that, the sensor chip was regenerated with 10mM Glycine-HCl pH 1,7. SPR analysis were performed with Biacore T200 instrument form GE Healthcare and data analysis was performed with Bioacore T200 Evaluation software 3.0 (GE Healthcare).

3.11. Transmission electron microscopy (TEM)

To visualize the FimHDG-NPs, negative staining electron microscopy was used technique. 5 ul of diluted sample (20 ng/microliter) were loaded onto a glow-discharged copper 300-square mesh grid for 30 seconds. The excess was blotted, and the grid was stained with Nano-W stain (Ted Pella, Inc.) for 30 seconds. Samples were then analyzed using the Tecnai G2 spirit and the images were acquired with Veleta CCD sensor.

3.12. Immunization scheme

Twelve CD1 female mice per group were immunized at day 0, 21 and 36 with 0,55 and 1,6 micrograms of recombinant protein expressed in bacterial or mammalian systems. AS01 was used as adjuvant. All mice were inoculated subcutaneously (SC) with 200µl of antigen + adjuvant (in PBS solution) or adjuvant alone as negative control for three times. Below in the table is reported the immunization scheme. Blood was collected through the tail vein at 0, 21, 36 and 49 days. Blood samples were spun to separate plasma (supernatant) and the rest of the whole blood. Upon heat inactivation at 56°C for 30 min, the plasma was further spun to remove precipitates.

Time points (days)	Activity	Material
-2	Urine collection form hydrophobic sand	Pre-immune urine
-1	Blood collection	Pre-immune sera
0	**Immunization I**	-
20	Blood collection	Post-I
21	**Immunization II**	-
34	Urine collection	Post-II
35	Blood collection	Post-II
36	**Immunization III**	-
48	Urine collection	Post-III
49	Blood collection and bloodletting	Post-III

Table 1. Immunization scheme

Animal work was approved by the local Animal Welfare Body, according to GSK Animal Welfare Policies and in compliance with national legislation/Ministry of Health

3.13. Enzyme-linked immunosorbent assay (ELISA)

Specific serum anti-FimHDG antibodies were measured by a classic enzyme-linked immunosorbent assay (ELISA). This is a standard technique; the protocol is briefly reported: 96-well microtiter Nunc Maxsorp plates were coated using 100µl of antigen concentrated 1µg/ml) for each well. Plates were then incubated overnight at 4°C. For each well, 250µl of polyvinylpyrrolidone (PVP) saturation buffer and the plates were then incubated for 2 hours at 37°C. All the wells were washed three times with PBS + Tween20 0,1% (PBT) and subsequently added with 100µl of diluted sera. Plates were then incubated at 37°C for 2 hours and washed again three times with PBT. 100µl of alkaline phosphate-conjugated anti-mouse secondary antibody serum diluted 1:2000 was added to each well. The plates were incubated 90 minutes at 37°C and then washed three times with PBT. Lastly, 100µl of p-nitrophenyl phosphate substrate were added and the plates were incubated at room temperature for 30 minutes. 100µl of 4N NaOH were added to each well and the signal was detected at 620-630nm absorbance.

3.14. Bacterial adhesion inhibition (BAI) assay

To test the functionality of the antibodies against FimH to inhibit bacterial adhesion, a BAI assay was performed. UTI89 wt_mCherry strain of *E. coli* was cultivated in three passages of static and liquid culture at 37°C to induce the expression of FimH. The assay was performed using a bacterial density of 0,012 OD/ml and incubation times of 30 minutes. Bacterial adhesion was measured by microscopy analysis using OPERA Phenix instrument. Epithelial cells SV-HUC obtained from ATCC were cultivated in SV-HUC complete medium composed by F12K from Thermo Scientific added with 10% of FBS and antibiotics (infection medium). In particular, 3 x T75 flasks of epithelial cells grown to 3 x 10^6 cells/ml were tripsinized for 5 minutes at 37°C and then seeded in 96-well plates with an initial cell count of 3,5 x 10^4 cells/well in a final volume of 200µl. Plates were incubated at 37°C with 5% of CO_2. The cell medium was then exchanged with 200µl of a medium that did not contain antibiotics (pre-infection medium). In the meanwhile, 2x solutions of sera were prepared in U-bottom 96-well plates with F12K medium or F12K + 10% FBS and further diluted with seral dilutions. To prepare the bacteria for the infection, 1mL of bacteria at their third passage were centrifuged at 4500g for 5 minutes, resuspended in PBS and pelleted. Finally, bacteria were resuspended at 0,5 OD600/ml in infection medium.

Infection protocol: for each plate, medium was removed and 50µl of 2x serum/mannose solution or infection medium (for positive and negative controls) together with 50µl of 2x inoculum or infection medium (negative control) were added to each well. Following an incubation of 30 minutes, serum dilution was added ranging from 15 to 0,06%. Plates were incubated again for 30 minutes at 37°C with 5% CO_2 then the medium was sucked off and the plates were washed three times with PBS. Bacteria were fixed with 200µl of 4% formaldehyde then, after an incubation of 20 minutes, formaldehyde was removed, and all the samples were washed with 200µl of PBS three times. 100µl of 1:5000 DAPI solution were added to each well and the plates were incubated 10 minutes at room temperature without direct light exposure. DAPI was removed and 200µl of PBS were added in each well, plates were then stored at 4°C in the dark and incubated 3 hours at room temperature before performing microscopy imaging with OPERA phenix.

Imaging settings: the whole well area was acquired using a 10x magnifying air objective with Alexafluor488 setting. 4 planes of Z-stack were acquired for each field and data were analyzed with Harmony Software. To have a value of adherence, the total bacterial fluorescence area was calculated.

4. Results

4.1. Computational structure-based design of stabilized monomeric FimH and FimH-stabilized nanoparticles

FimH has been used as vaccine candidate in complex with the periplasmic protein chaperone FimC. FimC component does not contribute to the FimH induced reduction of bacterial colonization in mice, rather in FimH stabilization from degradation. Importantly, FimC stabilizes FimH in its extended post-binding-like form [156]. However, it has been reported that the monoclonal antibodies against FimHL in the low affinity conformation lead to a better inhibition of adhesion to the bladder compared to antibodies against the mannose post-binding form [216].

In absence of FimC or its natural complementing FimG-donor strand, FimH is unstable and highly sensitive to periplasmic proteases [217, 218]. To produce a stable FimH, protein FimG donor strand peptide (FimG residues 1−14) has been added in vitro to displace the pilus assembly chaperone FimC from FimH [156] obtaining the FimH in the low affinity conformation. A low affinity conformation of recombinant FimHL domain has also been obtained inserting a disulphide bridge, locking the mannose pocket [219].

Our working hypothesis is that through a structure-guided design it is possible stabilize the pre-binding form of FimH in absence of FimC improving FimH immunogenicity. To design a stabilized, un-complexed full-length FimH the donor strand peptide from FimG, extrapolated from the pilus assembled crystal structure, was genetically fused through a linker of 4 or 5 amino acids, DNKQ and PGDGN respectively. This last linker was chosen because the initial Proline residue was predicted to support the turn in the secondary structure and to promote the correct folding of the donor strand in the architecture of FimH (Figure 9C). The linkers have been manually constructed, residue by residue trying to satisfy the criteria described in the material and methods section, locking the structure in the pre-binding conformation. The resulting construct was refined by a minimization process to relax the structure.

Giving the fact that the designed construct is a single chimeric sequence composed by the entire FimH and the donor strand from FimG, the chimeras were named FimH_PGDGN_DG and FimH_DNKQ_DG. The advantage of this approach relies on the fact that the entire stabilized antigen is encoded by one single nucleotide sequence, hence simplifying the expression, purification, and all

down-stream processes compared to the FimH-FimC candidate which requires two separate plasmids or a polycistronic gene.

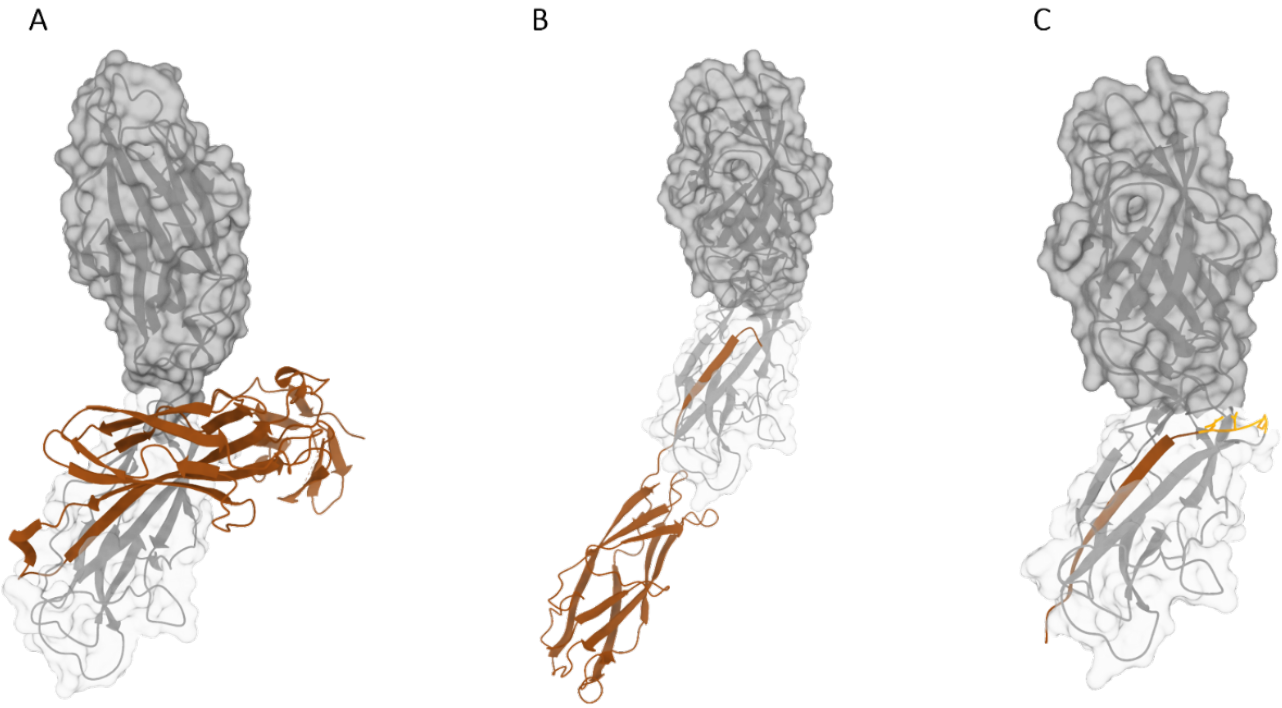

*Figure 9. Different strategies to stabilize FimH. Phase 2 vaccine candidate from Sequoia relies on the stabilization with periplasmic chaperone FimC (**A**) while in naturally assembled pilus FimH is stabilized by FimG donor strand complementation (**B**). Lastly, FimH can be stabilized by engineering the FimG donor strand into FimH sequence creating a "self-stabilized" chimera (**C**).* Molecule visualization and representation with UCSF ChimeraX software.

Another concern about the FimH-FimC vaccine candidate against ExPEC is its low immunogenicity in humans. The immunization protocol to elicit a robust immune response required 4 doses and this could represent a compliance problem [1]. To overcome this problem, we decided to explore the potentialities of self-assembling protein nanoparticles to increase the antigen immunogenicity and enable a 1-2 dose vaccine. For this study, three NPs with different geometries and number of subunits were selected: *Helicobacter pylori* ferritin (PDB 3BVE), mI3 (PDB 5KP9) and encapsulin (PDB 3DKT). While ferritin and encapsulin are naturally assembling into NPs, composed by 24 and 60 subunits respectively, mI3 is a computationally in silico designed 60-mer NP derived from the *Thermotoga marittima* 2-keto-3-deoxy-phosphogluconate (KDPG) aldolase and further improved by mutating two cysteine residues (table 2)[220, 221].

Protein based nanoparticles			
	Ferritin	**mI3**	**Encapsulin**
PDB code	3BVE	5DKT	3DKT
Organism	*H. pylori*	Computationally designed from *T. maritima*	*T. maritima*
Shape	Octahedral	Icosahedral	Icosahedral
Diameter (nm)	10	25	24
Subunits	24	60	60
MW (kDa)	15	25	32
MW NP (kDa)	360	1500	1920
Phase study	Clinical	Preclinical	Preclinical

Table 2. Summary of protein-based nanoparticles and virus like particles tested in this study. mI3 derives from the optimization of the I03 nanoparticle previously designed by Hsia et al. [35, 36]. The structures of mI3 and I03 have not been reported, consequently for the structural analysis a closely related icosahedral T. maritima particle (see PDB 5KP9) was used as a reference.

To correctly design the chimeric FimH-NPs, an accurate analysis of the crystal structures and the symmetry of the NPs was performed (figure 10). The structures were downloaded from the Protein Data Bank (PDB) and analysed using PyMOL as molecular visualization program. The structural analysis of each NP, reported in table 2, allowed the identification of potentially suitable sites for the insertion of the antigen. In detail, the C-terminal portion was oriented towards the inside of the NPs or involved in interface interactions necessary for the particle assembly. In contrast, the N-terminal portion was directed towards the outside of the NPs. Considering that, we decided that the N-terminal region was the most appropriate for antigen display, achievable by genetic engineering.

Based on the structural analysis above, the stabilized antigen was genetically fused at the N-terminus of each NP spaced by a linker composed of a repetition of Glycine and Serine residues [222, 223]. Internal to this linker, it was also inserted an 8xHis tag to allow a simpler protein purification.

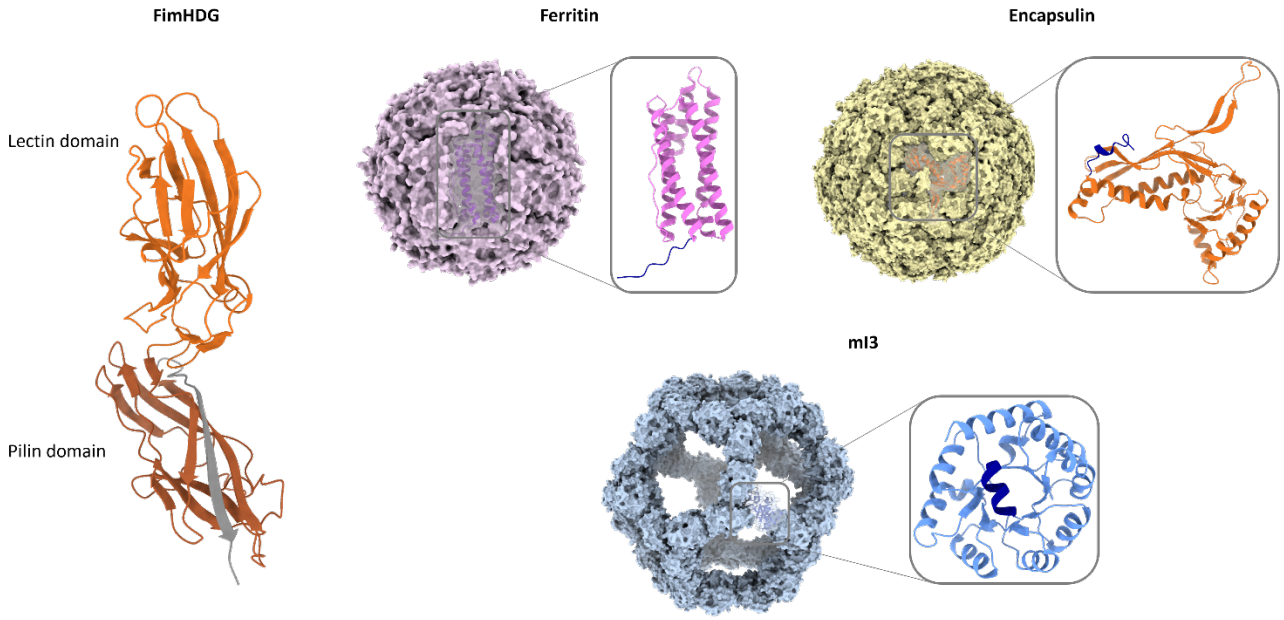

Figure 10. FimH stabilized with donor strand from FimG, named FimHDG (left) and selected nanoparticle to perform the multicopy display of the antigen (right). FimHDG is represented in cartoon with the pilin domain in dark orange and lectin domain in light orange. Donor strand form FimG is reported in grey. Ferritin, Encapsulin and mI3 nanoparticles are represented in surface highlighting the monomeric repeating unit (grey squares). Image was realised using ChimeraX software.

The designed chimeras were then analysed to assure that the spatial disposition of the antigen on the surface of the NP was correct (figure 11). To do this, the prediction of the 3D structure of the entire assembly was performed using Rosetta suite, and in particular the homology modelling method [224]. The alignments of sequences and structures of both NPs and antigen allowed the *in-silico* reconstruction of all predicted models. By analysing these models, we ensured that no steric clashes between the fused antigen were present when exposed at each vertex of the nanoparticles.

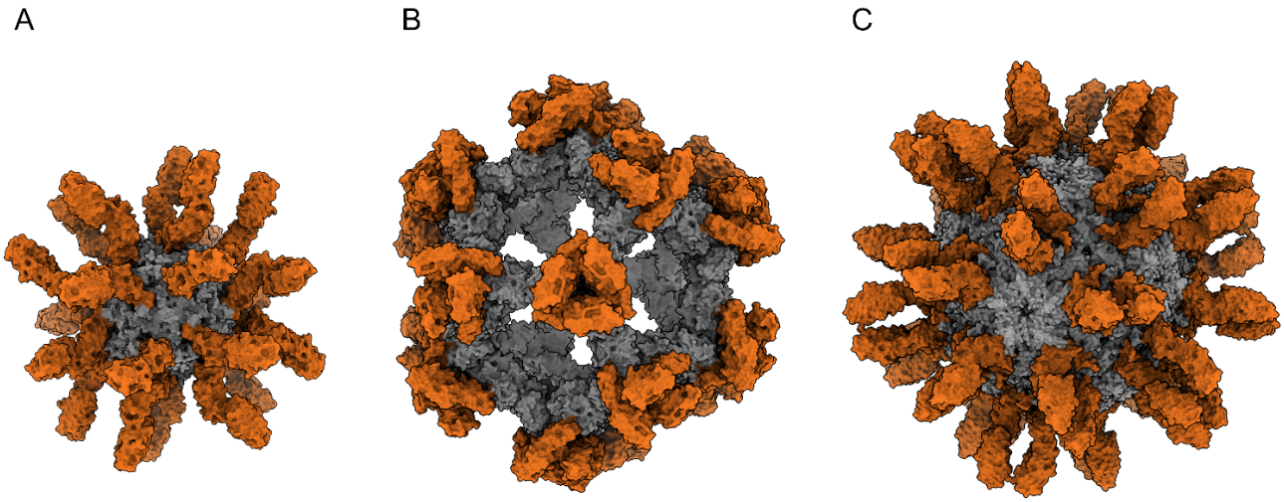

Figure 11. 3D reconstruction of NPs decorated with FimHDG realised using RosettaCM. In grey is represented the NP scaffold, in orange FimHDG. From left to right, *H. pylori* ferritin (**A**), mI3 (**B**), *T. maritima* Encapsulin (**C**). Molecule visualization and representation was performed with UCSF ChimeraX software.

4.2. Stabilized FimH proteins and FimH-FimC complex are secreted and easily purified from a mammalian expression system

Initially, the first attempts were focused on the expression of stabilized FimH and FimHDG-NPs in a bacterial expression system based on non-pathogenic *E. coli* since this approach would have granted a simple and low-cost method for recombinant protein production. To screen different conditions of expression, several parameters were taken into consideration such as the strength of the promoter used, the genetic background of the *E. coli* strain, the subcellular compartment where to express the recombinant proteins and the expression protocols, all summarized in table 3. For the cytoplasmic expression, two different promoters were tested: T7 and ptac using pET and pTrcHis2A vectors respectively. In the periplasm, different types of plasmids regulated by T7, T5, rhaBAD or araBAD promoters were tested. In both cases two expression protocols at lower temperatures (20 or 25°C) were tested with the objective to slow down the cell growth but at the same time increasing the solubility of the constructs. For the same reason, different *E. coli* strains, such as BL21(DE3), T7 Express lysY/Iq, T7 Express shuffle, BL21(SOLU) and W3110, were also tested.

Despite all the different conditions tested, none of the constructs resulted to be expressed in soluble form in *E. coli.* This would require complex and time-consuming *in vitro* purification. However, refolding often requires several attempts to achieve success and the entire process is time consuming and, often, recovered yields are low.

For these reasons, a mammalian expression system was considered as suitable to produce FimH_DG. In this case the protein does not accumulate inside the cells, but it is secreted in the medium and this could be particularly beneficial for FimH protein which contains two internal disulphide bonds which can be formed in the medium used for the cultivation. Here, pCDNA3.1 vector was used exploiting the leader sequence of the murine IgK chain for the secretion.

Expression system	Expression	Leader sequence	Vectors	Promoters	Temperatures	Strains
E. coli	Periplasmic	WT PelB	pacycDUET-1 pET22 pET303/CT-His	T7	20°C 25°C	BL21(DE3) BL21(SOLU) T7ExpressLysY/Iq W3110 T7 Shuffle
			pD404-NH-SR pD404-WR	T5		
			pD864-SR pD864-WR	rhaBAD		
			pBAD/Myc-HisA	araBAD		
	Cytoplasmic		pET22 pET303/CT-His pET24	T7		
			pTrcHis 2A	Trc with LacIq		
Mammalian	Secreted	IgK murine	pCDNA3.1	CMV		Expi293/GnTI, ExpiCHO

Table 3. Tested conditions for E. coli and mammalian recombinant protein expression.

Full length FimH stabilized with the donor strand from FimG containing the secretion leader sequence, alone or fused to NPs, were used to transfect Expi293 cells. The secretion of the proteins was characterized by assessing their expression in culture supernatants 3 and 6 days post transfection by Western Blot analysis. In (figure 12) it is reported the analysis of the expression of different FimH constructs stabilized with DNKQ or PGDGN linkers. FimH_ΔGG_PGDGN_DG, that bears a deletion of two glycine residues connecting FimHL and FimHP, was not expressed at 3 or 6 days after the transfection whereas both FimH_PGDGN_DG and FimH_DNKQ_DG well expressed and secreted in the medium. The expression of FimH-FimC complex as point of comparison with our chimeras was also tested. The complex resulted to be well expressed and, as well as for the other two constructs, the molecular weight of all the recombinant proteins expressed in mammalian cells was higher than expected. This can be explained by the differences in the glycosylation pattern that exist between bacteria and mammalian cells.

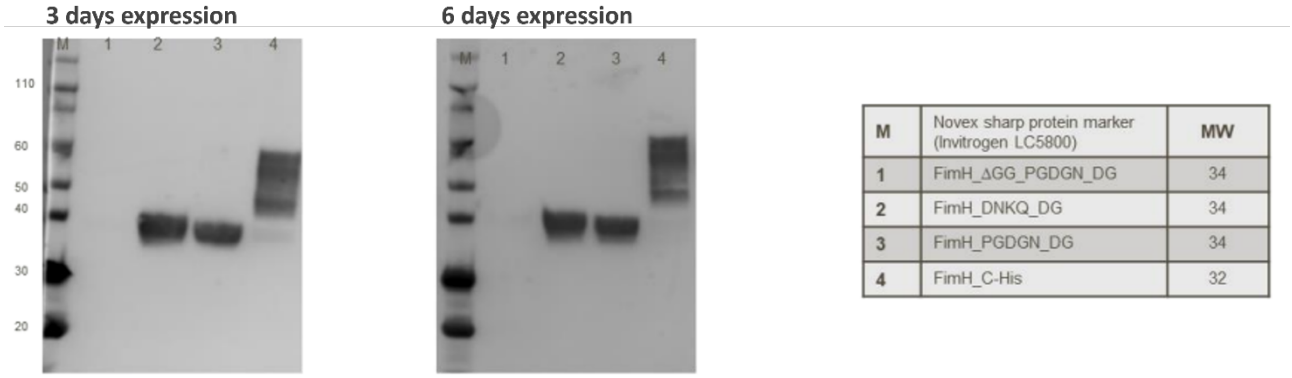

M	Novex sharp protein marker (Invitrogen LC5800)	MW
1	FimH_ΔGG_PGDGN_DG	34
2	FimH_DNKQ_DG	34
3	FimH_PGDGN_DG	34
4	FimH_C-His	32

Figure 12. Western blot analysis on Expi293 supernatants expressing different constructs of stabilized FimH 3 and 6 days after transfection. On the right is reported the loading order of the gels and the expected molecular weights. Western blot analysis was performed as described in material and methods section. The primary antibody used was an anti His-Tag HRP conjugated diluted 1:1000 v/v.

The expression of chimeric constructs was followed by their purification by immobilized metal ion affinity chromatography (IMAC) using the HiTrap TALON crude 5 mL column. This first step allowed to separate alle the non His-Tagged proteins present in the Expi293 growth medium from the proteins of interest. To assess the purity level, the proteins were analysed with by a size-exclusion and a reverse-phase ultra-performance liquid chromatography (SE-UPLC and RP-UPLC respectively). Purity was also assessed through SDS-Page analysis of the final collected proteins.

In figure 13A is reported the SDS-Page analysis on the purified FimH_PGDGN_DG samples. A very sharp signal is detected over 39 kDa, a higher molecular weight than expected, confirming the

probable presence of glycosylation on the protein. This data is confirmed by the SE-UPLC chromatogram reported in figure 13B where two distinct but not fully resolved peaks are visible at around 6.50- and 7-minutes of elution times witnessing the presence of two different glycosylated species. This assumption is also supported by the RP-UPLC, technique that is commonly used for the analysis and purification of peptides, proteins, and glycoproteins (figure 13C). In the chromatogram, obtained reading at 280nm, two distinct peaks are visible confirming that there are at least two differently glycosylated species in the analysed sample.

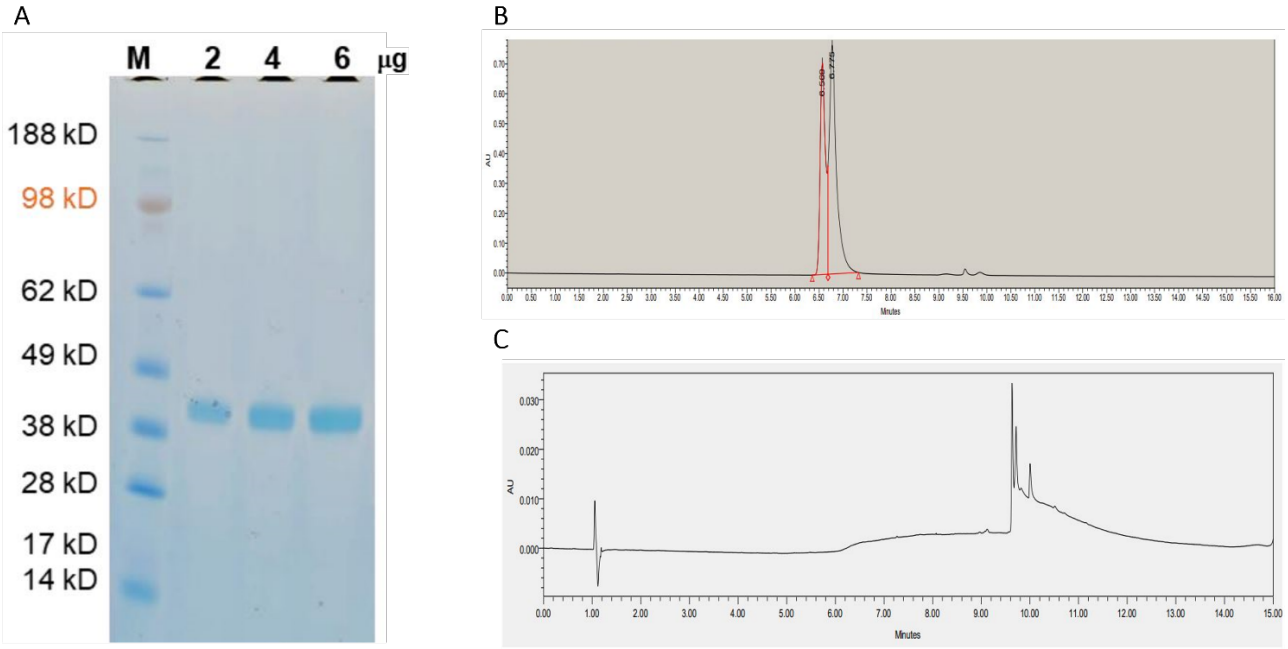

Figure 13. Purification and characterization of FimH_PGDGN_DG. A. SDS-Page analysis of purified sample loading 2, 4 and 6 µg of purified protein. B. SE-UPLC performed loading 15 µl of sample in a BEH200 4,6x300mm column (waters). C. RP-UPLC performed loading 50 µl of UPLC-purified sample in a Acquity UPLC Protein BEH C4 2,1x150 mm column.

FimH_DNKQ_DG shows very similar characteristics to FimH_PGDGN_DG. This is expected since this construct differs from FimH_PGDGN_DG just for the linker connecting the donor strand of FimG to FimH. In figure 14 are reported the data collected after the purification of the sample. The purification process followed the same workflow described before. The SDS-Page (figure 14A) analysis of the purified sample shows a band at a slightly higher molecular weight than the expected due to the probable presence of glycosylated species. As for the previous construct, the presence of glycosylation on FimH_DNKQ_DG was assessed by SE-UPLC and RP-UPLC. The chromatograms are reported in figure 14B and C respectively and in both cases is possible to appreciate two distinct peaks representing two differently glycosylated forms of FimH.

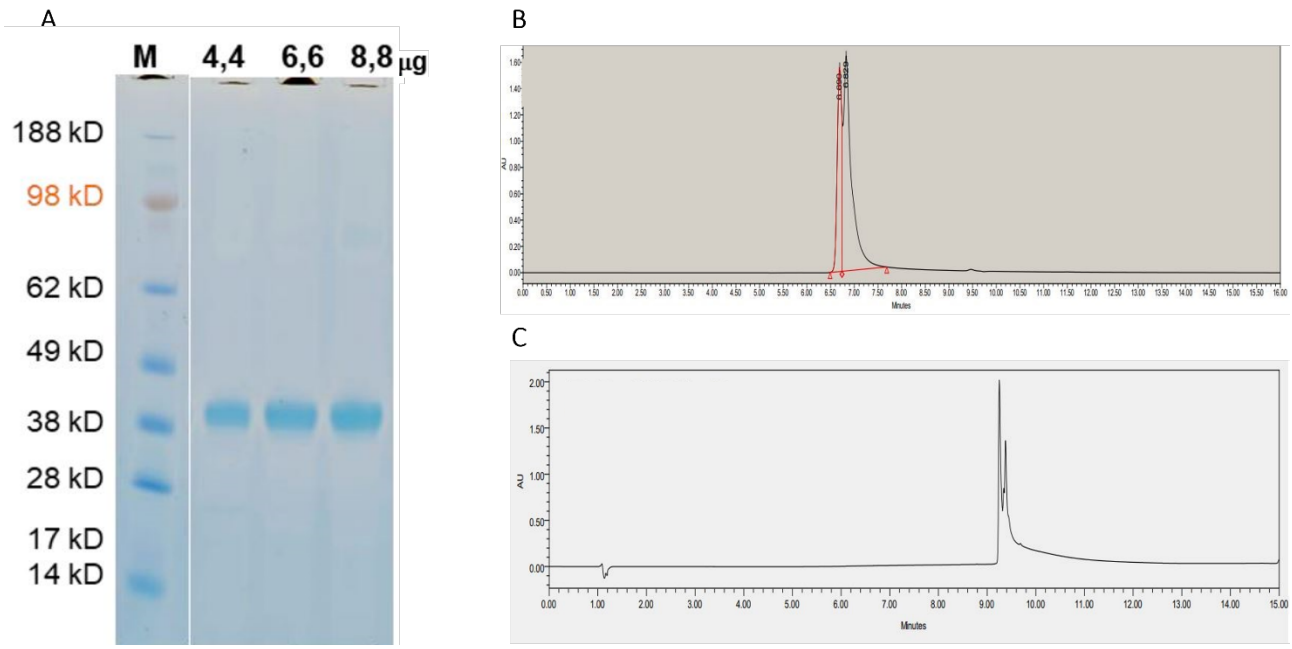

Figure 14. Purification and characterization of FimH_DNKQ_DG. A. SDS-Page analysis of purified sample loading 4,4, 6,6 and 8,8 µg of purified protein. B. SE-UPLC performed loading 15 µl of sample in a BEH200 4,6x300mm column (waters). C. RP-UPLC performed loading 50 µl of UPLC-purified sample in a Acquity UPLC Protein BEH C4 2,1x150 mm column.

4.3. The C-terminal His-tag does not affect the folding of stabilized FimH antigen

The purified samples were evaluated for their stability trhough differential scanning fluorimetry method, NanoSDF. This assay uses tryptophan or tyrosine fluorescence to monitor protein unfolding when a linear temperature ramp is applied and allows to determine the melting temperatue, Tm, that corresponds to the midpoint of the transition from folded to unfolded state.

In figure 15 is reported the data regarding the thermal stability of FimH_PGDGN_DG measured by NanoDSF, since FimH_DNKQ_DG showed a very similar behaviour, with slightly lower Tm, data are not shown. In both analysis the stability was assessed in presence or absence of 1M mannose to evaluate if the interaction between the protein and its ligand had a stabilizing effect. Melting temperatures are reported in figure 15; notably, there are no differencies in terms of stability between the samples with or without mannose. This could be explained by the fact that this chimeric FimH, stabilized by donor strand complementation, is “locked” in a low-affinity state for mannose and therefore is not able to avidly bind it. From the analysis it emerges that FimH_DG has two melting temperatures, probably corresponding to the two domains composing the protein. The first Tm, named Tm1 and , was assessed at 54°C while the second, Tm2, at 67°C.

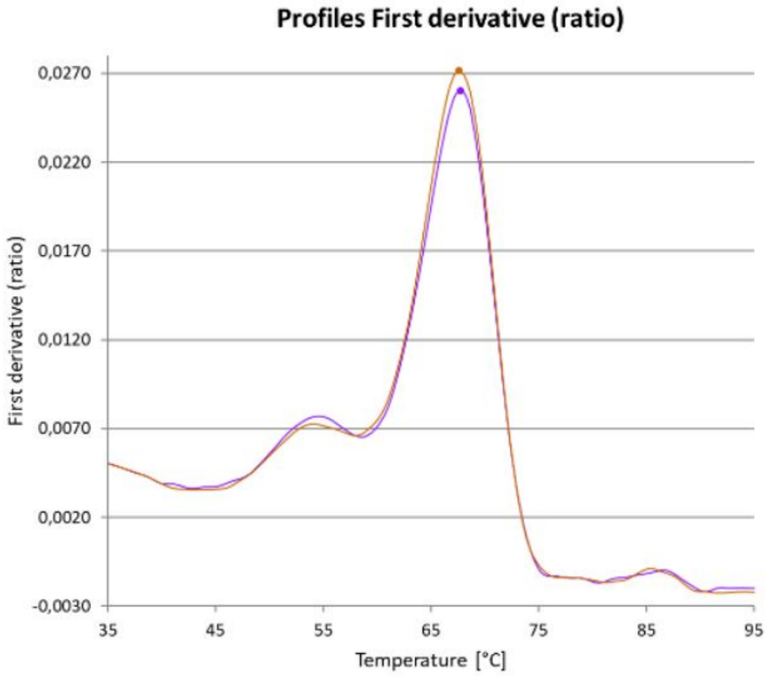

FimH_PGDGN_DG		
	Tm 1	**Tm 2**
No mannose	54°C	67°C
Mannose	54°C	67°C
Δ T°C	0°C	0°C

Figure 15. Thermal stability of FimH_PGDGN_DG evaluated by NanoDSF analysis. The Tm of each sample is calculated by finding the peak value of the first derivative.

To compare the structural stability of FimH_PGDGN_DG in presence and absence of the C-terminal His-tag a construct deprived of the 6 histidine residues was designed and named FimH_PGDGN_DG_tagless. In figure 16 is reported the stability profile of FimH_PGDGN_DG tagless expressed in Expi293. In the table are reported the precise Tm values. It is possible to note that for the thermal stability profile is very similar to the one reported above meaning that the overall folding and stability of FimH is not affected by the His tag. Similarly to the His-tagged construct, the tagless stabilized FimH_DG shows two melting temperatures, the first one at 56°C, representing the unfolding of the first domain, and the second at 74°C, representing the second domain. The same experiment was performed on the tagless construct expressed in the CHO mammalian cell line to evaluate if any difference due to the different glycosylation pattern was present. Even when expressed in another cell line, the stability profile of FimH remains unchanged (data not shown), meaning that the protein is stable and properly folded even when expressed in different conditions with or without His tag.

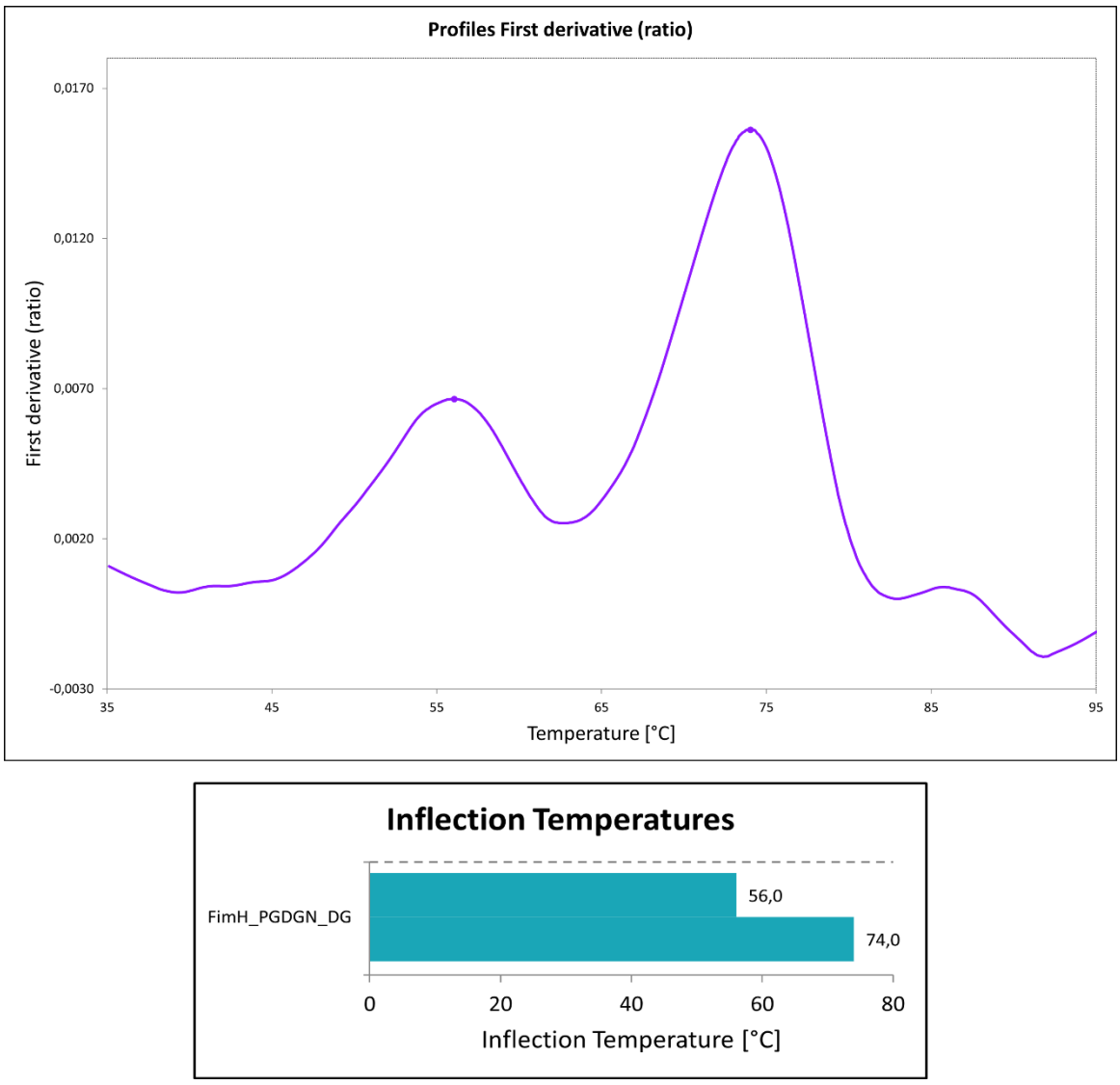

Figure 16. NanoDSF profiles and melting temperature obtained for FimH_PGDGN_DG tagless expressed in Expi293. The table reports the two inflection points represented as peaks when considering the first derivative of the curve.

4.4. Chimeric FimH_PGDGN_DG-Nanoparticles are secreted and correctly assembled when expressed in mammalian cells

Since the PGDGN linker resulted in a higher stabilization of FimH compared to the DNKQ linker, *H. pylori* ferritin, mI3 and encapsulin nanoparticles were used to design chimeric NPs exposing on their surface this stabilized FimH construct, from now on called FimHDG.

The strategy to express the selected NPs in a bacterial system has been proven to work in previous studies, for this reason the first attempts to express the chimeric FimHDG-nanoparticles were made in bacterial strains. However, none of the constructs resulted to be soluble when expressed in *E. coli*,

confirming the data obtained from the expression of FimH_DG as single recombinant antigen. In figure 17A is reported the SDS-Page analysis of the bacterial expression in BL21(DE3) of FimDG-Ferritin nanoparticle. The construct is expressed and visible as a 52 kDa band in the total fraction after cell lysis. After centrifugation the soluble fraction was recovered and run on SDS-PAGE to assess the presence of the target construct in the soluble fraction (lane 2, figure 17A). Notably, no signal appeared at the expected molecular weight, indicating a high propensity of the protein to accumulate in the inclusion bodies. The pellet containing the inclusion bodies obtained from the previous centrifugation step was then resuspended with a buffer containing urea 6M. The sample was centrifugated and the supernatant was run on the gel. The resulting pellet was finally resuspended with a buffer containing urea 8M and an aliquot was run. These steps were made to disrupt and to resolubilize the inclusion bodies containing the protein of interest. As indicated by the blue star, after the resuspension with urea 8M an intense band at 52 kDa appeared on the gel, indicating that although the construct is well expressed in the bacterial strain, it is not soluble, and it accumulates in the inclusion bodies.

To achieve soluble protein expression, the mammalian expression system was tested. Ferritin and mI3 have been successfully expressed in mammalian system to display viral antigens. Two different mammalian cell lines, Expi293 and ExpiCHO. As described before, the chimeric constructs were engineered to carry the Igk murine leader sequence for the secretion in the growth medium. The C-terminal His-tag of monomeric single FimHDG was substituted by a flexible glycine-serine linker that allowed the two interconnected proteins, nanoparticle and FimHDG, to move freely. the SDS-Page analysis on the supernatants of Expi293 cells after 5 days from transfection is reported (figure 17B). As highlighted by the blue stars all three constructs were expressed and present in growth medium. As observed for the mammalian produced FimHDG alone, the three constructs run at a slightly higher molecular weight than expected due to the presence of glycosylation compared to the bacterial expression. Since this strategy allowed us to obtain soluble chimeric FimHDG-NPs, the mammalian expression system was chosen to produce the antigens over the bacterial one, that would have required more purification steps.

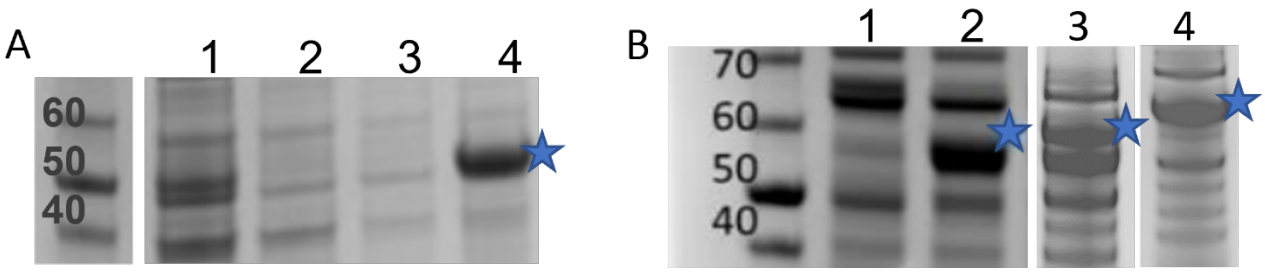

1	Total extract
2	Soluble fraction
3	Wash 6M Urea
4	Solubilized 8M Urea

1	Expi293 not transfected
2	FimHDG-Ferrtin
3	FimHDG-mI3
4	FimHDG-Encapsulin

Sample	a.a.	Expected M.W. (kDa)
FimHDG-Ferritin	493	52,7
FimHDG-mI3	538	56,8
FimHDG-Encapsulin	598	65,2

Figure 17. SDS-Page analysis of FimHDG-NPs expression in two different expression systems. A. Expression in BL21(DE3) led to accumulation of the chimeric protein in inclusion bodies (lane 4) while in the soluble fraction no protein of interest was detected. B. Expi293 mammalian cell line expression system led to the expression and secretion of all three constructs. Aminoacidic length and expected molecular weight expressed in kDa are reported in the table at the bottom.

Following the expression, Expi293 supernatants containing the three chimeric nanoparticles were recovered, filtered with 0,22µm filters and concentrated by centrifugation with 300 kDa Amicon filters. The concentrated samples were then purified by SEC using a Superose 6 10/300 column GL, able to separate molecules ranging from 5 to 5000 kDa. In figure 18A are reported the chromatograms of the three FimHDG-NPs. As highlighted by the red arrow, a sharp peak at the expected elution volume is present in all three samples, suggesting the presence of high molecular weight particles. The fractions corresponding to the correct peak were recovered, pooled, and run on an SDS-Page gel to evaluate the purity of the samples (figure 18B). A single band corresponding to the molecular weight of the monomers is present confirming that the column was able to purify the fraction corresponding to the correctly assembled nanoparticle.

An additional confirmation that FimHDG-ferritin, FimHDG-mI3 and FimHDG-encapsulin form correctly assembled and stable NPs was given by visualizing the purified samples using negative stain transmission electron microscopy (TEM). As shown in figure 18C, all three nanoparticles appeared as differentially oriented homogeneous populations of particles decorated by spikes. The length of

these spikes (8,5 nm) corresponds exactly to the theorical length of FimHDG calculated on the model witnessing that all NPs expose on their surface the chimeric antigen.

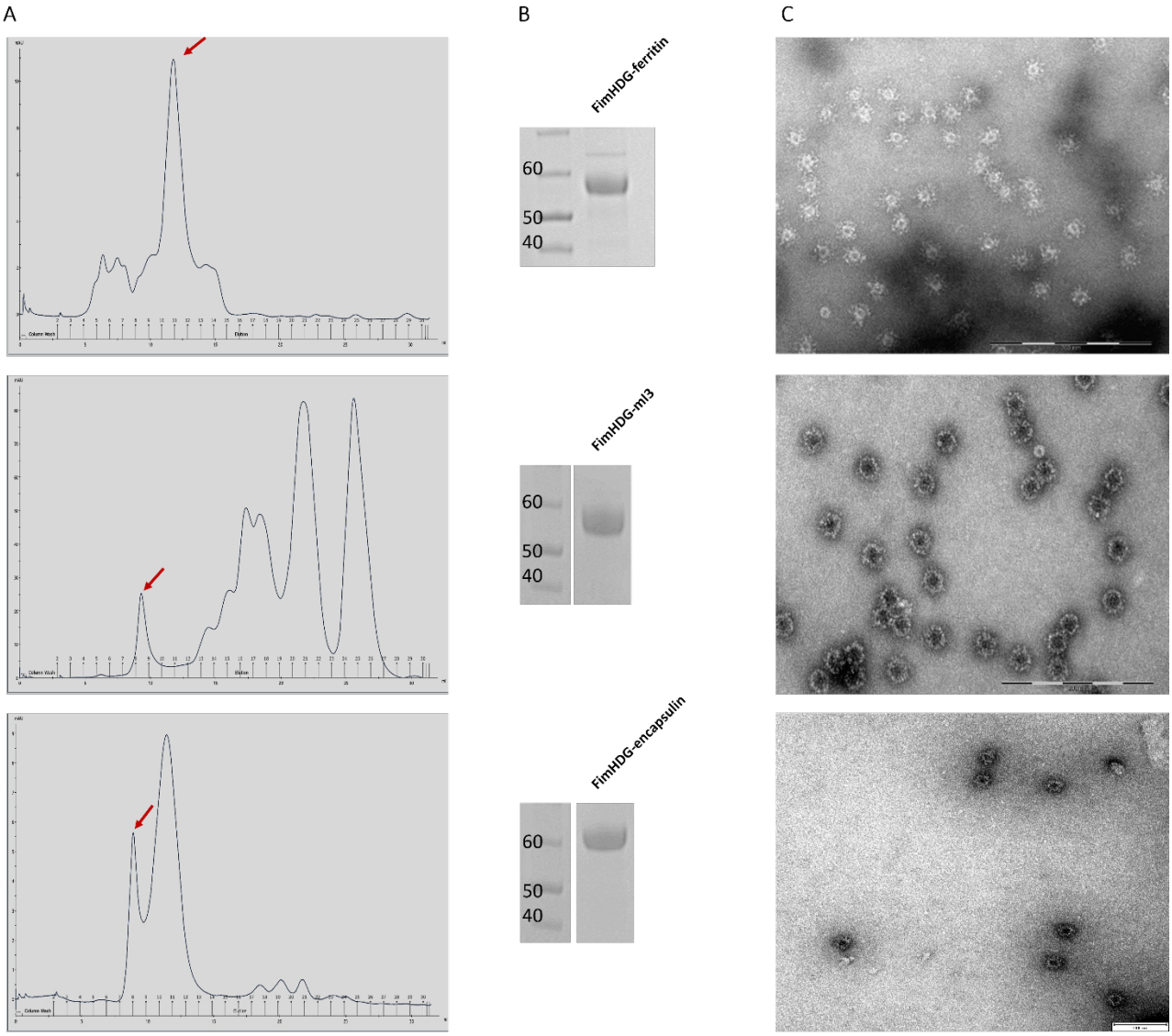

Figure 18. Purification and visualization of FimHDG-NPs. ***A****. SEC chromatograms of ferritin (top), mI3 (middle), and encapsulin (bottom) decorated with FimHDG, red arrows indicate the peaks that eluted at the expected elution volume using a Superose 6 10/300 GL column.* ***B.*** *SDS-Page analysis performed on the recovered pooled fractions. 20 µl of boiled sample were loaded on the gel.* ***C.*** *TEM imaging of the purified nanoparticles. Ferritin (top), mI3 (middle), and encapsulin (bottom) appear as circular entities decorated with FimHDG visible as spikes on the NPs surface. Scalebar reported in the TEM pictures correspond to 200nm for FimHDG-Ferritin NPs and 100nm for FimHDG-mI3 and Encapsulin NPs.*

4.5. FimHDG folding and stability is not affected by the display on nanoparticles

Another aspect to consider when working with chimeric constructs is the impact that the genetic fusion can have their folding and stability. To address this question, a NanoDSF assay was performed on the three FimHDG-NPs and the analysis of the first derivative of the fluorescence signal is reported in figure 19. Analysing the first derivative allows us to better appreciate the melting temperatures at which the lectin and pilin domains of FimHDG unfold while it is not possible to appreciate a melting temperature for any nanoparticles their melting temperature is too high to be detected by this technique. As expected, the first FimH domain to unfold is the lectin domain followed by the pilin domain, this characteristic stability profile is in agreement with the one observed for the FimHDG protein alone and is compatible with the 3D structure of the protein, suggesting that the antigen maintains its structural properties when displayed on a NP. Compared to the single recombinant antigen, FimHDG fused on a NP shows a slightly higher Tm for both domains as reported in the table. This effect could be due to the high stability of the carrier that reflects also on the antigen on its surface. FimHDG fused to mI3 and ferritin shows higher Tm values for the pilin domain (Tm2 76,6°C) while the lectin domain seems more stable when FimHDG is displayed on the encapsulin (Tm1 61,5°C). Despite these little variations, no substantial differences in the stability profile were noted among the FimHDG displayed on the three NPs, witnessing that the genetic fusion on the nanoparticles is not compromising the three-dimensional fold of the antigen.

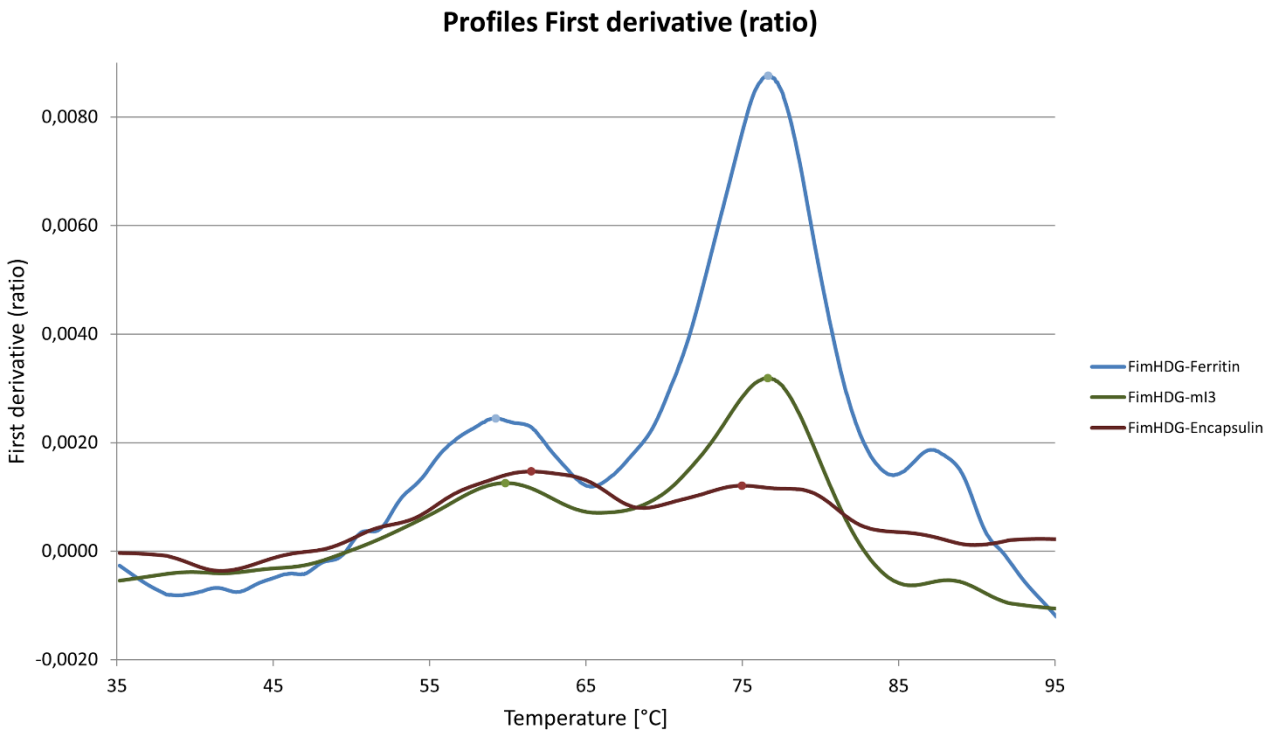

	FimHDG-Ferritin	FimHDG-mI3	FimHDG-Encapsulin
Tm 1	59,2°C	59,8°C	61,5°C
Tm 2	76,6°C	76,6°C	75°C

Figure 19. NanoDSF profiles and melting temperatures obtained for FimHDG-Ferritin (blue), FimHDG-mI3 (green), and FimHDG-Encapsulin (brown).

4.6. FimH stabilized with FimG donor strand is locked in the pre-binding conformation as demonstrated by the binding to mAb926

To study which conformation the lectin domain of FimHDG adopted upon its stabilization with the FimG donor strand, an SPR analysis using mAb926 was performed. This monoclonal antibody was described to bind the lectin domain when the loops involved in the interaction with the mannose are in a pre-binding conformation [135]. Since this is the state that we sought to stabilize, the binding to this antibody would be the proof of the correct structural conformation of the antigen. In figure 20 is reported the sensorgram obtained by analysing different monomeric FimH constructs and FimHDG-Ferritin nanoparticle. Notably, while FimHDG expressed from bacterial or mammalian systems (pink and green lines respectively) showed similar binding profiles to the monoclonal antibody, with differences in the association and dissociation profiles. These differences can be explained by the fact that the stabilization induced by FimC leads to a post-binding conformation that does not allow a strong binding with the selected antibody. By contrast, FimHDG-Ferritin (blue line) resulted to bind

more stably to the antibody. This is in part expected since the simultaneous multicopy display of the antigen on the nanoparticle can explain the increased avidity observed. . Taken together, these data confirm that the stabilization of FimH with the donor strand from FimG leads to a pre-binding conformation stabilized construct.

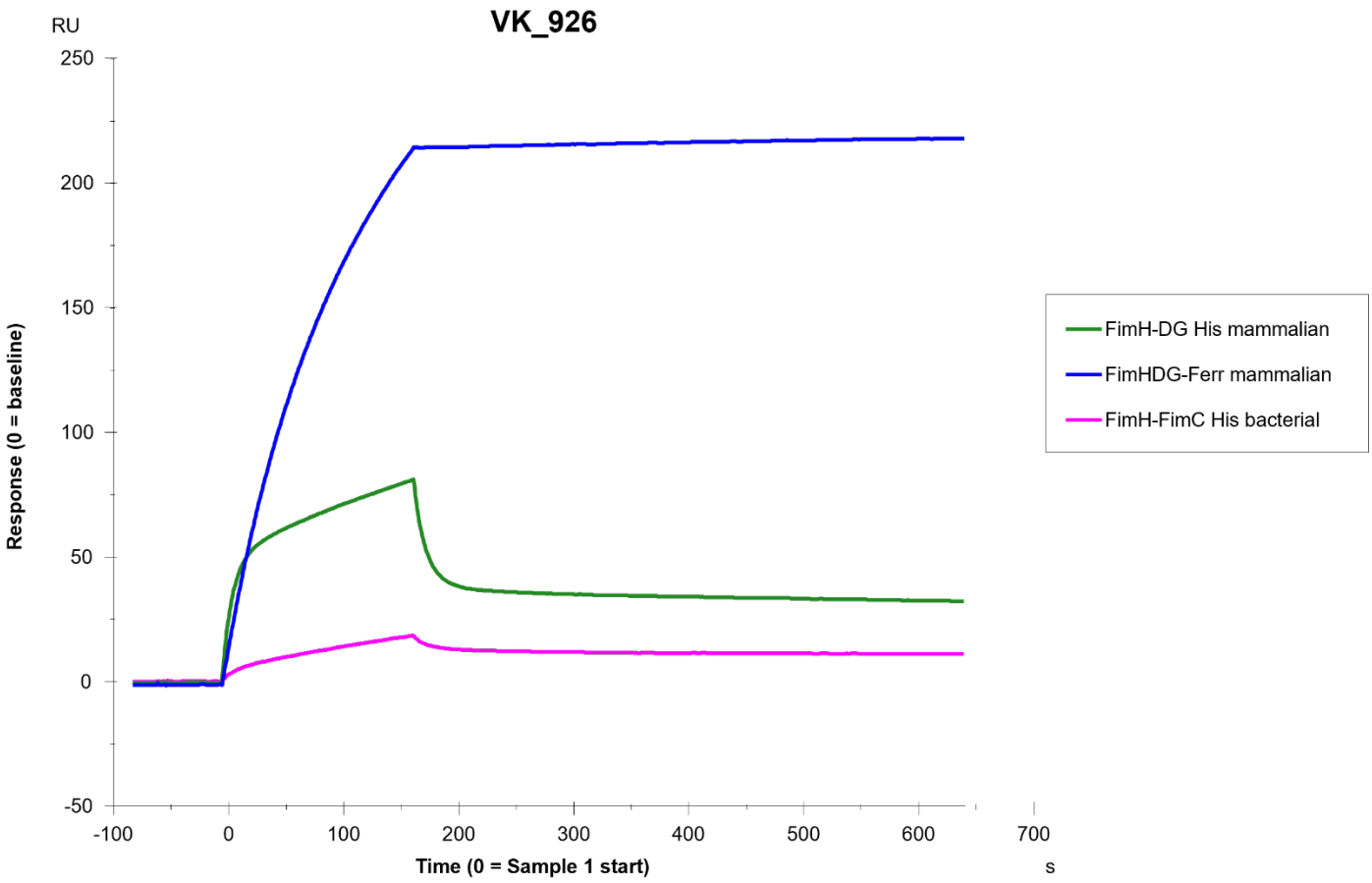

Sample	mAb	Binding level [RU]
FimH-FimC (Bacterial)	VK 926	21,4
FimHDG His (Mammalian)	VK 926	81,8
FimHDG-Ferr (Mammalian)	VK 926	200,2

Figure 20. SPR analysis of different FimH constructs interacting with mAb926. The sensorgram reports the response (y axis) against the time (x axis) measured in Resonance Units (RU). The association phase, first part of the graph, describes the interaction between the two analytes while the second part describes the dissociation between the two species.

4.7. Recombinant FimHDG stabilized antigen and FimHDG-Ferritin are highly immunogenic in mouse

The immune response elicited by FimHC (FimH-FimC) complex and FimH stabilized candidates, including FimH-Ferritin nanoparticle, was assessed by immunizing mice with 0,5 and 1,6µg of antigen adjuvated with PHAD (as used in the clinical trial) or AS01. The immunization scheme is reported in the section Materials and Methods. FimH-specific serum IgG titers after the second (post-II) and third (post-III) injection were evaluated by enzyme-linked immunosorbent assay (ELISA) and are reported in figure 21. Total IgG titres values of FimHDG produced in the mammalian system was compared with those elicited by FimHC complex produced in bacteria as benchmark. At 0,55µg antigen dose there is a clear enhancement of the antibody response with FimHDG produced as single recombinant antigen in a mammalian system and adjuvated with AS01 over the FimHC complex adjuvated with PHAD. For what it concerns the FimHDG-Ferritin construct, it was able to elicit a stronger immune response compared to both FimHC complex and FimHDG recombinant antigen. In this case in fact, both 0,55 and 1,6µg of mammalian FimHDG-Ferritin induced a response that plateaued after the 2nd and 3rd immunization also showing a less scattered response.

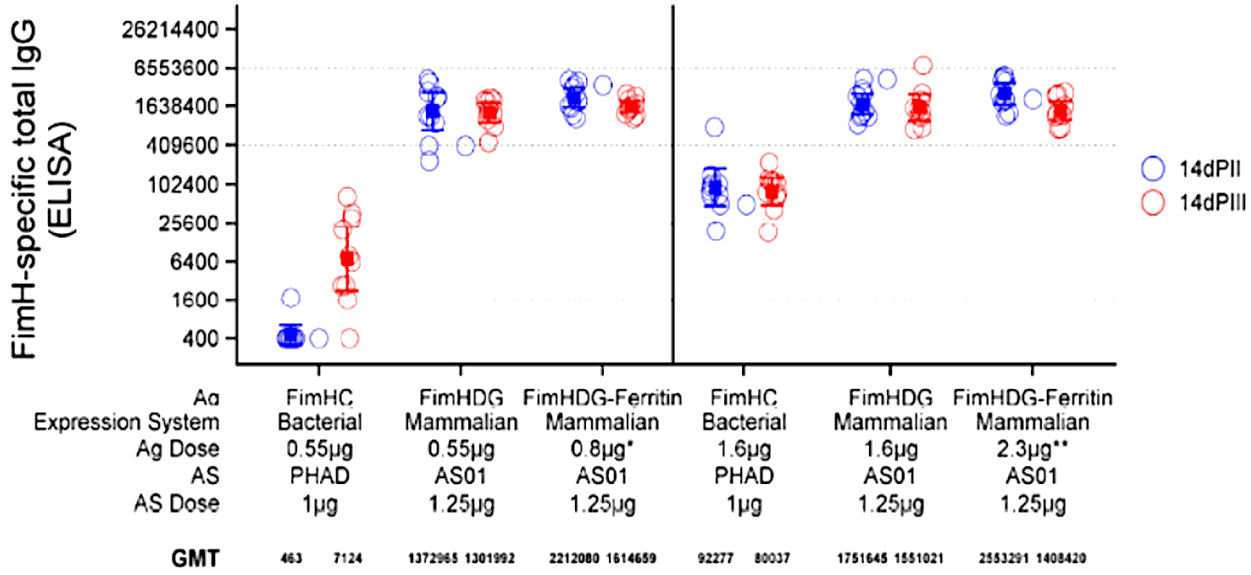

Figure 21. FimH-specific total IgG evaluation by ELISA analysis. Different stabilized FimH constructs from mammalian and bacterial expression systems were evaluated for their ability to elicit an immune response in mouse. The antibody titers were assumed to be lognormally distributed and geometric mean titers (GMTs) were calculated. Statistical analyses were performed using SAS 9.4.

4.8. FimHDG and FimHDG-Ferritin candidates have a stronger capability to inhibit bacterial adhesion compared to FimHC benchmark

To evaluate the anti-FimH antibody ability to inhibit uropathogenic *E. coli* adhesion to uroepithelial cells, a bacterial inhibition assay (BAI) was performed. Here, sera derived from immunization with FimHDG and FimHC complex were plated at different concentration to estimate the dose-response curve. The titre is expressed in Relative Potency (RP) and is obtained from the comparison between the tested sample against the reference serum. In figure 22 are reported the results describing antibody functionality assessed through the BAI assay. These data reveal that sera raised against both FimHDG (orange) and FimHDG-Ferritin (pink) expressed in the mammalian expression system have a stronger ability to inhibit bacterial adhesion compared to sera raised against FimHC (black). Furthermore, sera raised against FimHDG-Ferritin using the lower dose of antigen (0,55μg) showed at least a 10-fold higher functionality compared to those raised against FimHDG expressed as a single recombinant antigen in mammalian cells. This data show that FimH stabilized in a pre-binding conformation can elicit a stronger and more functional immune response compared to the post-binding conformation. The contribution of the multicopy display allowed by the nanoparticle size and geometry also plays an important role in eliciting more functional antibodies compared to the single recombinant antigen; this effect is particularly visible at lower doses, where the display on the nanoparticle raises sera that are 10-fold more effective in inhibiting the bacterial adhesion compared to the single antigen, while at higher doses (1,6 μg) this effect is less accentuated with the FimHDG-Ferritin showing a 1,4 fold higher functionality compared to FimHDG.

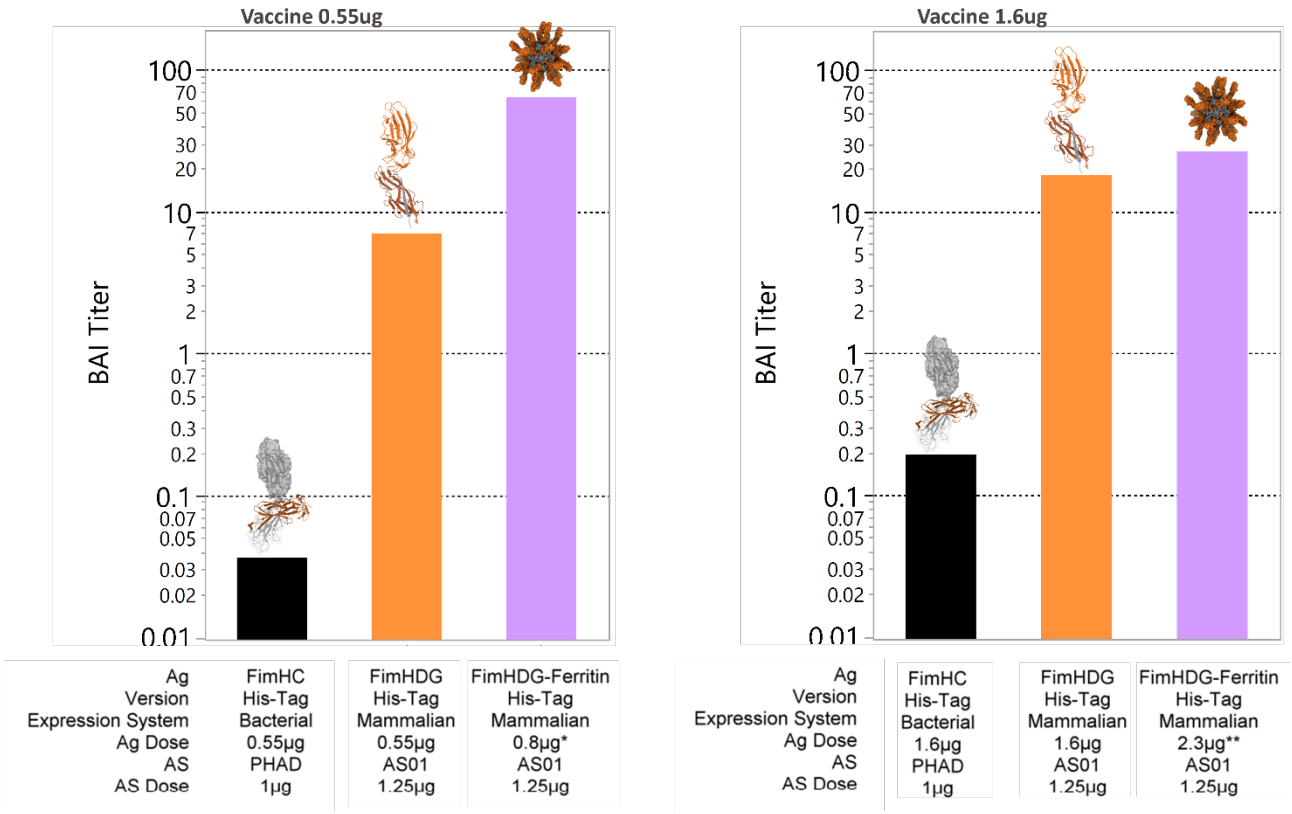

Figure 22. Bacterial adhesion inhibition assay performed on sera raised against FimHC complex expressed in bacteria (black bar), FimHDG His tag expressed in mammalian (orange bar) and FimHDG-Ferritin expressed in mammalian (pink bar). A lower (0.55µg) and higher (1,6µg) antigen doses were tested and a comparison between the samples wad made. PHAD and AS01 were used as adjuvants.

5. Discussion and future perspectives

UTIs are amongst the most common bacterial infections worldwide and a major cause of hospitalization [35]. The widespread dissemination of these infections raises the need of the development of an effective vaccine that, to date, is still missing on the market. Although it is quite difficult to keep track of the pathogens causing UTIs, it is estimated that *E. coli* is responsible for more than a half of these infections [26-29]. This data, together with the emerging antibiotic resistance problem, makes *E. coli* a major target for the development of new vaccines and therapies alternatives to the antibiotic treatment [18].

In this context we identified the highly conserved adhesin FimH as a suitable antigen for the development of a vaccine candidate able to cover the majority of antibiotic resistant strains of uropathogenic *E. coli* [141]. Targeting the distal tip of the pilus would allow to develop an immune response and functional antibodies able to prevent the adhesion, hence the colonization and the infection, of the bacterium to the surface of urothelium present in the low urinary tract [225].

To date, only few vaccines were developed against this pathogen and all of them lack efficacy or required several doses to elicit a strong immune response, posing serious concerns about the compliance of the prophylaxis [226].

For these reasons, we investigated an innovative strategy to stabilize the tip protein of the type I pilus, FimH, to be used then as a vaccine candidate to prevent urinary tract infections caused by ExPEC strains. This strategy relies on the stabilization that naturally occurs when FimG complements the structure of FimH by a mechanism called donor strand complementation [227]. Here a β strand of FimG completes and stabilizes the structure of the pilin domain of FimH. Since this phenomenon just requires a β strand from FimG, we reasoned that the stabilization could occur even if the donor strand was genetically fused at the C-terminal domain of FimH, spaced by a properly designed linker. This strategy led to a “one-step” stabilization of FimH without the need of ancillary elements, such as FimC or FimG, to be co-expressed along with the antigen of interest.

The first approach to express the stabilized version of FimH has been *E. coli*, since it represents a cost effective and relatively easy way to express recombinant proteins. Despite several attempts of cytoplasmic and periplasmic expression, it was not possible to obtain a soluble and well folded protein. In fact, FimHDG tends to accumulate in the E. coli cytoplasmic space as inclusion bodies made of unfolded aggregated protein that would require a complex purification strategy in order to obtain a well folded final product. Several attempts were made to obtain soluble protein, changing expression promoter and the expression cell line, as T7 shuffle cells which are suitable for the

production of protein with internal disulphide bonds. The periplasmic expression was also explored as it has been successful for the soluble production of the FimH-FimC complex. However, even if different leader sequences have been tested, soluble expression has not been achieved. For these reasons the expression in mammalian cell lines has been also explored. In this case the FimH_DG protein was engineered with a leader sequence that allows its secretion into the growth medium. The expression in different cell lines, including Expi293 and CHO, led to the expression of soluble and correctly folded recombinant proteins, as witnessed by SDS-Page, SEC, and NanoDSF analysis performed on the purified recombinant protein. In particular, the thermal stability analysis revealed that the stabilized FimH fold correctly into a two-domain protein with very similar melting temperatures when compared with the wild-type stabilized FimH.

Once assessed that the stabilization strategy through the genetic fusion worked and allowed us to obtain a correctly folded version of FimH, we decided to explore the potentialities of the self-assembling protein nanoparticles to repetitively display the antigen and hopefully boost its immunogenicity. Three nanoparticles described in literature as suitable for genetic fusion and antigen display were selected based on their dimension, geometry, and possibility to engineer them. Based on the crystal structures of the nanoparticles, we genetically fused the antigen at the N-terminus of each monomer since this is the most flexible and solvent-exposed region. To validate the structure-based design, we predicted the 3D models of each chimeric nanoparticle using Rosetta Comparative Modelling Suite; these models revealed that the antigens are correctly exposed on the surface of each nanoparticle, avoiding clashes or steric hindrance.
Based on these preliminary results, we expressed the FimH-nanoparticles constructs in mammalian cells obtaining soluble secreted proteins. After a purification step, we characterized the correct assembly of the nanoparticle through size exclusion chromatography, dynamic light scattering and negative staining electron microscopy techniques. In all cases we could assess that the nanoparticles were correctly assembled and homogeneous, furthermore they correctly exposed the correctly folded antigen on their surfaces as witnessed by the surface plasmon resonance analysis. From this analysis it resulted also that the nanoparticles increase the binding stability of FimH to the conformational monoclonal antibody mAb926 compared to the single recombinant protein; this phenomenon can be explained by the repetitive display of the antigen on the surface of a geometrically defined nanoparticle.

After the physical and biochemical characterization, we performed an *in vivo* study conducted in mice to compare the immunogenicity of the recombinant stabilized FimH and the FimH-nanoparticles to

the currently used FimH-FimC complex as a benchmark. The study revealed that FimH stabilized with the donor strand from FimG using the genetic fusion approach is significantly more immunogenic and able to generate a more functional immune response compared to the benchmark. Furthermore, the use of ferritin scaffold for the display of FimH resulted in a 10-fold increase of antigen immunogenicity compared to the stabilized monomeric antigen. Moreover, the elicited antibodies resulted to be able to inhibit bacterial adhesion in an *in vitro* assay called BAI.

This study proposes a new strategy to produce a stabilized construct of FimH. This stabilization is based on the genetic fusion of the donor strand form FimG, and the construct tend to be and more immunogenic and functional compared to the benchmark. Furthermore, we designed and successfully expressed three chimeric NPs exposing the stabilized FimH construct on the surface with the aim to improve the immunogenic profile of the antigen. In particular, we were able to successfully express and purify these bacterial derived proteins using a mammalian expression system while the bacterial expression led to expression of insoluble proteins. This strategy opens a series of questions that are yet to be fully investigated, such as the role of the mammalian glycosylation on the immunogenicity of the recombinant proteins and the scalability of the process in terms of production costs. Additionally, being able to express these bacterial candidates in an eukaryotic system pave the way to investigate other eukaryotic systems such as yeast or insect cells (i.e. baculovirus expression system) that are already used in to scale up the production of recombinant proteins.
In conclusion, this study sets the stage for the development of an effective vaccine against urinary tract infections caused by ExPEC.

Table 4. Aminoacidic sequences used in this study

Protein name	Expected A.A. Sequence
FimH-FimC complex	**FimH**: MKRVITLFAVLLMGWSVNAWSFACKTANGTAIPIGGGSAN VYVNLAPVVNVGQNLVVDLSTQIFCHNDYPETITDYVTLQ RGSAYGGVLSNFSGTVKYSGSSYPFPTTSETPRVVYNSRTD KPWPVALYLTPVSSAGGVAIKAGSLIAVLILRQTNNYNSDD FQFVWNIYANNDVVVPTGGCDVSARDVTVTLPDYPGSVPI PLTVYCAKSQNLGYYLSGTTADAGNSIFTNTASFSPAQGVG VQLTRNGTIIPANNTVSLGAVGTSAVSLGLTANYARTGGQ VTAGNVQSIIGVTFVYQ **FimC**: MSNKNVNVRKSQEITFCLLAGILMFMAMMVAGRAEAGVA LGATRVIYPAGQKQVQLAVTNNDENSTYLIQSWVENADG VKDGRFIVTPPLFAMKGKKENTLRILDATNNQLPQDRESLF WMNVKAIPSMDKSKLTENTLQLAIISRIKLYYRPAKLALPP DQAAEKLRFRRSANSLTLINPTPYYLTVTELNAGTRVLENA LVPPMGESTVKLPSDAGSNITYRTINDYGALTPKMTGVME GSGHHHHHH
FimH_DNKQ_DG	METDTLLLWVLLLWVPGSTGDFACKTANGTAIPIGGGSAN VYVNLAPVVNVGQNLVVDLSTQIFCHNDYPETITDYVTLQ RGSAYGGVLSNFSGTVKYSGSSYPFPTTSETPRVVYNSRTD KPWPVALYLTPVSSAGGVAIKAGSLIAVLILRQTNNYNSDD FQFVWNIYANNDVVVPTGGCDVSARDVTVTLPDYPGSVPI PLTVYCAKSQNLGYYLSGTTADAGNSIFTNTASFSPAQGVG VQLTRNGTIIPANNTVSLGAVGTSAVSLGLTANYARTGGQ VTAGNVQSIIGVTFVYQDNKQADVTITVNGKVVAKGSGHH HHHH
FimH_PGDGN_DG	METDTLLLWVLLLWVPGSTGDFACKTANGTAIPIGGGSAN VYVNLAPVVNVGQNLVVDLSTQIFCHNDYPETITDYVTLQ RGSAYGGVLSNFSGTVKYSGSSYPFPTTSETPRVVYNSRTD KPWPVALYLTPVSSAGGVAIKAGSLIAVLILRQTNNYNSDD FQFVWNIYANNDVVVPTGGCDVSARDVTVTLPDYPGSVPI

	PLTVYCAKSQNLGYYLSGTTADAGNSIFTNTASFSPAQGVG VQLTRNGTIIPANNTVSLGAVGTSAVSLGLTANYARTGGQ VTAGNVQSIIGVTFVYQPGDGNADVTITVNGKVVAKGSGH HHHHH
FimH_ΔGG_PGDGN_DG	METDTLLLWVLLLWVPGSTGDFACKTANGTAIPIGGGSAN VYVNLAPVVNVGQNLVVDLSTQIFCHNDYPETITDYVTLQ RGSAYGGVLSNFSGTVKYSGSSYPFPTTSETPRVVYNSRTD KPWPVALYLTPVSSAGGVAIKAGSLIAVLILRQTNNYNSDD FQFVWNIYANNDVVVPTCDVSARDVTVTLPDYPGSVPIPLT VYCAKSQNLGYYLSGTTADAGNSIFTNTASFSPAQGVGVQ LTRNGTIIPANNTVSLGAVGTSAVSLGLTANYARTGGQVTA GNVQSIIGVTFVYQPGDGNADVTITVNGKVVAKGSGHHHH HH
FimHDG-Ferritin	METDTLLLWVLLLWVPGSTGDFACKTANGTAIPIGGGSAN VYVNLAPAVNVGQNLVVDLSTQIFCHNDYPETITDYVTLQ RGSAYGGVLSSFSGTVKYNGSSYPFPTTSETPRVVYNSRTD KPWPVALYLTPVSAGGVAIKAGSLIAVLILRQTNNYNSDDF QFVWNIYANNDVVVPTGGCDVSARDVTVTLPDYPGSVPIP LTVYCAKSQNLGYYLSGTTADAGNSIFTNTASFSPAQGVG VQLTRNGTIIPANNTVSLGAVGTSAVSLGLTANYARTGGQ VTAGNVQSIIGVTFVYQPGDGNADVTITVNGKVVAKGGSG GSGGSGGSDIIKLLNEQVNKEMNSSNLYMSMSSWCYTHSL DGAGLFLFDHAAEEYEHAKKLIIFLNENNVPVQLTSISAPEH KFEGLTQIFQKAYEHEQHISESINNIVDHAIKSKDHATFNFL QWYVAEQHEEEVLFKDILDKIELIGNENHGLYLADQYVKG IAKSRK
FimHDG-mI3	METDTLLLWVLLLWVPGSTGDFACKTANGTAIPIGGGSAN VYVNLAPAVNVGQNLVVDLSTQIFCHNDYPETITDYVTLQ RGSAYGGVLSSFSGTVKYNGSSYPFPTTSETPRVVYNSRTD KPWPVALYLTPVSSAGGVAIKAGSLIAVLILRQTNNYNSDD FQFVWNIYANNDVVVPTGGCDVSARDVTVTLPDYPGSVPI PLTVYCAKSQNLGYYLSGTTADAGNSIFTNTASFSPAQGVG VQLTRNGTIIPANNTVSLGAVGTSAVSLGLTANYARTGGQ

	VTAGNVQSIIGVTFVYQPGDGNADVTITVNGKVVAKSGSH HHHHHHHGGSMKMEELFKKHKIVAVLRANSVEEAKKKAL AVFLGGVHLIEITFTVPDADTVIKELSFLKEMGAIIGAGTVT SVEQARKAVESGAEFIVSPHLDEEISQFAKEKGVFYMPGV MTPTELVKAMKLGHTILKLFPGEVVGPQFVKAMKGPFPNV KFVPTGGVNLDNVCEWFKAGVLAVGVGSALVKGTPVEVA EKAKAFVEKIRGCTE
FimHDG-Encapsulin	METDTLLLWVLLLWVPGSTGDFACKTANGTAIPIGGGSAN VYVNLAPAVNVGQNLVVDLSTQIFCHNDYPETITDYVTLQ RGSAYGGVLSSFSGTVKYNGSSYPFPTTSETPRVVYNSRTD KPWPVALYLTPVSSAGGVAIKAGSLIAVLILRQTNNYNSDD FQFVWNIYANNDVVVPTGGCDVSARDVTVTLPDYPGSVPI PLTVYCAKSQNLGYYLSGTTADAGNSIFTNTASFSPAQGVG VQLTRNGTIIPANNTVSLGAVGTSAVSLGLTANYARTGGQ VTAGNVQSIIGVTFVYQPGDGNADVTITVNGKVVAKSGSH HHHHHHHGGSMEFLKRSFAPLTEKQWQEIDNRAREIFKTQ LYGRKFVDVEGPYGWEYAAHPLGEVEVLSDENEVVKWGL RKSLPLIELRATFTLDLWELDNLERGKPNVDLSSLEETVRK VAEFEDEVIFRGCEKSGVKGLLSFEERKIECGSTPKDLLEAI VRALSIFSKDGIEGPYTLVINTDRWINFLKEEAGHYPLEKRV EECLRGGKIITTPRIEDALVVSERGGDFKLILGQDLSIGYEDR EKDAVRLFITETFTFQVVNPEALILLKF

Conflict of interest: Paolo Cinelli is a PhD student at University of Bologna and participates in a post graduate studentship program at GSK. This work was sponsored by GlaxoSmithKline Biologicals SA which was involved in all stages of the study conduct and analysis also supporting the preparation and the publication of the manuscript.

1. Eldridge, G.R., et al., *Safety and immunogenicity of an adjuvanted Escherichia coli adhesin vaccine in healthy women with and without histories of recurrent urinary tract infections: results from a first-in-human phase 1 study.* (2164-554X (Electronic)).
2. Tenaillon, O., et al., *The population genetics of commensal Escherichia coli.* Nature Reviews Microbiology, 2010. **8**(3): p. 207-217.
3. Stenutz, R., G. Weintraub A Fau - Widmalm, and G. Widmalm, *The structures of Escherichia coli O-polysaccharide antigens.* (0168-6445 (Print)).
4. Fratamico, P.M., et al., *Advances in Molecular Serotyping and Subtyping of Escherichia coli.* (1664-302X (Print)).
5. Whitfield, C., *Biosynthesis and assembly of capsular polysaccharides in Escherichia coli.* (0066-4154 (Print)).
6. Kaczmarek, A., A. Budzyńska, and E. Gospodarek, *Detection of K1 antigen of Escherichia coli rods isolated from pregnant women and neonates.* Folia Microbiologica, 2014. **59**(5): p. 419-422.
7. Geue, L., et al., *Rapid microarray-based DNA genoserotyping of Escherichia coli.* (1348-0421 (Electronic)).
8. Poolman, J.T. and M. Wacker, *Extraintestinal Pathogenic Escherichia coli, a Common Human Pathogen: Challenges for Vaccine Development and Progress in the Field.* (1537-6613 (Electronic)).
9. Leimbach, A., U. Hacker J Fau - Dobrindt, and U. Dobrindt, *E. coli as an all-rounder: the thin line between commensalism and pathogenicity.* (0070-217X (Print)).
10. Nesta, B. and M. Pizza, *Vaccines Against Escherichia coli.* (0070-217X (Print)).
11. Dobrindt, U., *(Patho-)Genomics of Escherichia coli.* (1438-4221 (Print)).
12. Ochman, H., J.G. Lawrence, and E.A. Groisman, *Lateral gene transfer and the nature of bacterial innovation.* Nature, 2000. **405**(6784): p. 299-304.
13. Brzuszkiewicz E Fau - Gottschalk, G., et al., *Adaptation of Pathogenic E. coli to Various Niches: Genome Flexibility is the Key.* (1660-9263 (Print)).
14. Frank, C., et al., *Large and ongoing outbreak of haemolytic uraemic syndrome, Germany, May 2011.* 2011. **16**(21): p. 19878.
15. Nordstrom, L., L.B. Liu Cm Fau - Price, and L.B. Price, *Foodborne urinary tract infections: a new paradigm for antimicrobial-resistant foodborne illness.* (1664-302X (Print)).
16. Tacconelli, E., et al., *Discovery, research, and development of new antibiotics: the WHO priority list of antibiotic-resistant bacteria and tuberculosis.* The Lancet Infectious Diseases, 2018. **18**(3): p. 318-327.
17. Shah, C., et al., *Virulence factors of uropathogenic Escherichia coli (UPEC) and correlation with antimicrobial resistance.* (1471-2180 (Electronic)).
18. Zhen, X., et al., *Economic burden of antibiotic resistance in ESKAPE organisms: a systematic review.* Antimicrobial Resistance & Infection Control, 2019. **8**(1): p. 137.
19. Mazzariol, A., A. Bazaj, and G. Cornaglia, *Multi-drug-resistant Gram-negative bacteria causing urinary tract infections: a review.* Journal of Chemotherapy, 2017. **29**(sup1): p. 2-9.
20. Russo, T.A. and J.R. Johnson, *Medical and economic impact of extraintestinal infections due to Escherichia coli: focus on an increasingly important endemic problem.* (1286-4579 (Print)).
21. Pendleton, J.N., B.F. Gorman Sp Fau - Gilmore, and B.F. Gilmore, *Clinical relevance of the ESKAPE pathogens.* (1744-8336 (Electronic)).
22. Russo, T.A. and J.R. Johnson, *Medical and economic impact of extraintestinal infections due to Escherichia coli: focus on an increasingly important endemic problem.* Microbes and Infection, 2003. **5**(5): p. 449-456.
23. Manges Amee, R., et al., *Global Extraintestinal Pathogenic Escherichia coli (ExPEC) Lineages.* Clinical Microbiology Reviews. **32**(3): p. e00135-18.

24. Pendleton, J.N., S.P. Gorman, and B.F. Gilmore, *Clinical relevance of the ESKAPE pathogens.* Expert Rev Anti Infect Ther, 2013. **11**(3): p. 297-308.
25. Zhen, X., et al., *Economic burden of antibiotic resistance in ESKAPE organisms: a systematic review.* Antimicrob Resist Infect Control, 2019. **8**: p. 137.
26. Edelsberg, J., et al., *Prevalence of antibiotic resistance in US hospitals.* (1879-0070 (Electronic)).
27. Laupland, K.B. and D.L. Church, *Population-based epidemiology and microbiology of community-onset bloodstream infections.* (1098-6618 (Electronic)).
28. Williamson, D.A., et al., *Population-based incidence and comparative demographics of community-associated and healthcare-associated Escherichia coli bloodstream infection in Auckland, New Zealand, 2005-2011.* (1471-2334 (Electronic)).
29. Roubaud Baudron, C., et al., *Escherichia coli bacteraemia in adults: age-related differences in clinical and bacteriological characteristics, and outcome.* (1469-4409 (Electronic)).
30. Roberts, A.W., et al., *The population 65 years and older in the United States: 2016*. 2018: US Department of Commerce, Economics and Statistics Administration, US ….
31. Jackson, L.A., et al., *Burden of community-onset Escherichia coli bacteremia in seniors.* (0022-1899 (Print)).
32. Plos, K., et al., *Intestinal carriage of P fimbriated Escherichia coli and the susceptibility to urinary tract infection in young children.* (0022-1899 (Print)).
33. Turck M Fau - Petersdorf, R.G. and R.G. Petersdorf, *The epidemiology of nonenteric Escherichia coli infections: prevalence of serological groups.* (0021-9738 (Print)).
34. Alqasim A Fau - Scheutz, F., et al., *Comparative genome analysis identifies few traits unique to the Escherichia coli ST131 H30Rx clade and extensive mosaicism at the capsule locus.* (1471-2164 (Electronic)).
35. Stamm, W.E. and S.R. Norrby, *Urinary tract infections: disease panorama and challenges.* (0022-1899 (Print)).
36. Foxman, B., *Urinary tract infection syndromes: occurrence, recurrence, bacteriology, risk factors, and disease burden.* (1557-9824 (Electronic)).
37. Zilberberg, M.D. and A.F. Shorr, *Secular trends in gram-negative resistance among urinary tract infection hospitalizations in the United States, 2000-2009.* (1559-6834 (Electronic)).
38. Loveday, H.P., et al., *epic3: national evidence-based guidelines for preventing healthcare-associated infections in NHS hospitals in England.* (1532-2939 (Electronic)).
39. Laupland, K.B., et al., *Community-onset urinary tract infections: a population-based assessment.* (0300-8126 (Print)).
40. Mabeck, C.E., *Treatment of uncomplicated urinary tract infection in non-pregnant women.* (0032-5473 (Print)).
41. Medina, M. and E. Castillo-Pino, *An introduction to the epidemiology and burden of urinary tract infections.* Therapeutic advances in urology, 2019. **11**: p. 1756287219832172-1756287219832172.
42. Renard, J., et al., *Recurrent Lower Urinary Tract Infections Have a Detrimental Effect on Patient Quality of Life: a Prospective, Observational Study.* (2193-8229 (Print)).
43. Foxman, B., *Urinary Tract Infection Syndromes: Occurrence, Recurrence, Bacteriology, Risk Factors, and Disease Burden.* Infectious Disease Clinics of North America, 2014. **28**(1): p. 1-13.
44. Gupta, K., et al., *Inverse association of H2O2-producing lactobacilli and vaginal Escherichia coli colonization in women with recurrent urinary tract infections.* (0022-1899 (Print)).
45. Nicolas-Chanoine, M.H., X. Bertrand, and J.Y. Madec, *Escherichia coli ST131, an intriguing clonal group.* (1098-6618 (Electronic)).
46. Mathers, A.J., G. Peirano, and J.D. Pitout, *Escherichia coli ST131: The quintessential example of an international multiresistant high-risk clone.* (0065-2164 (Print)).

47. Ronald, A.R., et al., *Urinary tract infection in adults: research priorities and strategies.* (0924-8579 (Print)).
48. Mobley Harry, L.T., et al., *Uropathogenic Escherichia coli.* EcoSal Plus, 2009. **3**(2).
49. Hooton, T.M., *Clinical practice. Uncomplicated urinary tract infection.* (1533-4406 (Electronic)).
50. Levison, M.E. and D. Kaye, *Treatment of complicated urinary tract infections with an emphasis on drug-resistant gram-negative uropathogens.* (1523-3847 (Print)).
51. Lichtenberger, P. and T.M. Hooton, *Complicated urinary tract infections.* (1523-3847 (Print)).
52. Ki, M., et al., *The epidemiology of acute pyelonephritis in South Korea, 1997–1999.* 2004. **160**(10): p. 985-993.
53. Laupland, K., et al., *Community-onset urinary tract infections: a population-based assessment.* 2007. **35**(3): p. 150-153.
54. Foxman, B. and P.J.I.D.C. Brown, *Epidemiology of urinary tract infections: transmission and risk factors, incidence, and costs.* 2003. **17**(2): p. 227-241.
55. Craig, J.C., et al., *Antibiotic prophylaxis and recurrent urinary tract infection in children.* 2009. **361**(18): p. 1748-1759.
56. Foxman, B., et al., *Risk factors for second urinary tract infection among college women.* 2000. **151**(12): p. 1194-1205.
57. Drekonja, D.M., et al., *Urinary tract infection in male veterans: treatment patterns and outcomes.* 2013. **173**(1): p. 62-68.
58. Khandelwal, P., G. Abraham Sn Fau - Apodaca, and G. Apodaca, *Cell biology and physiology of the uroepithelium.* (1522-1466 (Electronic)).
59. Matuszewski, M.A., et al., *Uroplakins and their potential applications in urology.* (2080-4806 (Print)).
60. Flores-Mireles, A.L., et al., *Urinary tract infections: epidemiology, mechanisms of infection and treatment options.* (1740-1534 (Electronic)).
61. Niveditha, S., et al., *The Isolation and the Biofilm Formation of Uropathogens in the Patients with Catheter Associated Urinary Tract Infections (UTIs).* (2249-782X (Print)).
62. Donlan, R.M. and J.W. Costerton, *Biofilms: survival mechanisms of clinically relevant microorganisms.* (0893-8512 (Print)).
63. Warren, J.J.U.t.i.m.p. and W. clinical management. ASM Press, DC, *Clinical presentations and epidemiology of urinary tract infections.* 1996: p. 3-27.
64. Tenaillon, O., et al., *The population genetics of commensal Escherichia coli.* (1740-1534 (Electronic)).
65. Gal-Mor, O. and B.B. Finlay, *Pathogenicity islands: a molecular toolbox for bacterial virulence.* (1462-5814 (Print)).
66. Terlizzi, M.E., G. Gribaudo, and M.E. Maffei, *UroPathogenic Escherichia coli (UPEC) Infections: Virulence Factors, Bladder Responses, Antibiotic, and Non-antibiotic Antimicrobial Strategies.* (1664-302X (Print)).
67. Buckles, E.L., et al., *Role of the K2 Capsule in Escherichia coli Urinary Tract Infection and Serum Resistance.* The Journal of Infectious Diseases, 2009. **199**(11): p. 1689-1697.
68. Russo, T.A., et al., *Capsular polysaccharide and the O-specific antigen impede antibody binding: a potential obstacle for the successful development of an extraintestinal pathogenic Escherichia coli vaccine.* (0264-410X (Print)).
69. O'Hanley, P., et al., *Molecular basis of Escherichia coli colonization of the upper urinary tract in BALB/c mice. Gal-Gal pili immunization prevents Escherichia coli pyelonephritis in the BALB/c mouse model of human pyelonephritis.* The Journal of Clinical Investigation, 1985. **75**(2): p. 347-360.

70. Roberts Ja Fau - Hardaway, K., et al., *Prevention of pyelonephritis by immunization with P-fimbriae.* (0022-5347 (Print)).
71. Carnoy, C. and S.L. Moseley, *Mutational analysis of receptor binding mediated by the Dr family of Escherichia coli adhesins.* (0950-382X (Print)).
72. Goluszko, P., et al., *Vaccination with purified Dr Fimbriae reduces mortality associated with chronic urinary tract infection due to Escherichia coli bearing Dr adhesin.* (0019-9567 (Print)).
73. Zhou, G., et al., *Uroplakin Ia is the urothelial receptor for uropathogenic Escherichia coli: evidence from in vitro FimH binding.* 2001. **114**(22): p. 4095-4103.
74. Aronson M Fau - Medalia, O., et al., *Prevention of colonization of the urinary tract of mice with Escherichia coli by blocking of bacterial adherence with methyl alpha-D-mannopyranoside.* (0022-1899 (Print)).
75. Langermann, S., et al., *Prevention of mucosal Escherichia coli infection by FimH-adhesin-based systemic vaccination.* (0036-8075 (Print)).
76. van Regenmortel, M., *Vaccine design: Innovative Approaches and Novel Strategies Edited by Rino Rappuoli and Fabio Bagnoli (2011): Caister Academic Press, Norfolk, UK, 380 pages. ISBN :978-1-904455-74-5, Hardcover. $319 from Amazon.com. LID - 1493.* (0304-8608 (Print)).
77. Nielubowicz, G.R. and H.L.T. Mobley, *Host–pathogen interactions in urinary tract infection.* Nature Reviews Urology, 2010. **7**(8): p. 430-441.
78. Rippere-Lampe, K.E., et al., *Cytotoxic necrotizing factor type 1-positive Escherichia coli causes increased inflammation and tissue damage to the prostate in a rat prostatitis model.* Infect Immun, 2001. **69**(10): p. 6515-9.
79. Smith, Y.C., et al., *Hemolysin of uropathogenic Escherichia coli evokes extensive shedding of the uroepithelium and hemorrhage in bladder tissue within the first 24 hours after intraurethral inoculation of mice.* Infect Immun, 2008. **76**(7): p. 2978-90.
80. Stamm, W.E., *Scientific and clinical challenges in the management of urinary tract infections.* (0002-9343 (Print)).
81. Foxman, B., *The epidemiology of urinary tract infection.* Nature Reviews Urology, 2010. **7**(12): p. 653-660.
82. Foxman, B., *The epidemiology of urinary tract infection.* Nat Rev Urol, 2010. **7**(12): p. 653-60.
83. Foxman, B., et al., *Condom use and first-time urinary tract infection.* (1044-3983 (Print)).
84. Foxman, B., et al., *Risk factors for second urinary tract infection among college women.* (0002-9262 (Print)).
85. Bailey Rr Fau - Peddie, B.A., et al., *Sexual acquisition of urinary tract infection in a man.* (1660-8151 (Print)).
86. Schaberg Dr Fau - Weinstein, R.A., W.E. Weinstein Ra Fau - Stamm, and W.E. Stamm, *Epidemics of nosocomial urinary tract infection caused by multiply resistant gram-negative bacilli: epidemiology and control.* (0022-1899 (Print)).
87. Hooton, T.M., et al., *Diagnosis, Prevention, and Treatment of Catheter-Associated Urinary Tract Infection in Adults: 2009 International Clinical Practice Guidelines from the Infectious Diseases Society of America.* Clinical Infectious Diseases, 2010. **50**(5): p. 625-663.
88. Huang, W.C., et al., *Catheter-associated urinary tract infections in intensive care units can be reduced by prompting physicians to remove unnecessary catheters.* (0899-823X (Print)).
89. Blango, M.G. and M.A. Mulvey, *Persistence of uropathogenic Escherichia coli in the face of multiple antibiotics.* (1098-6596 (Electronic)).
90. Schito, G.C., et al., *The ARESC study: an international survey on the antimicrobial resistance of pathogens involved in uncomplicated urinary tract infections.* (1872-7913 (Electronic)).

91. Karlowsky, J.A., et al., *Trends in antimicrobial resistance among urinary tract infection isolates of Escherichia coli from female outpatients in the United States.* (0066-4804 (Print)).
92. Moreira, E.D., Jr., et al., *Antimicrobial resistance of Escherichia coli strains causing community-acquired urinary tract infections among insured and uninsured populations in a large urban center.* (1973-9478 (Electronic)).
93. Zhanel, G.G., et al., *Antibiotic resistance in outpatient urinary isolates: final results from the North American Urinary Tract Infection Collaborative Alliance (NAUTICA).* (0924-8579 (Print)).
94. Idil, N., et al., *High trimethoprim-sulfamethoxazole resistance in ciprofloxacin-resistant Escherichia coli strains isolated from urinary tract infection.* 2016. **28**(3).
95. Saha, S., et al., *Antimicrobial resistance in uropathogen isolates from patients with urinary tract infections.* 2015. **2**(5): p. 1-7.
96. Moya-Dionisio, V., et al., *[Uropathogen pattern and antimicrobial susceptibility in positive urinary cultures isolates from paediatric patients].* (1988-9518 (Electronic)).
97. Chang, U.I., H.W. Kim, and S.H. Wie, *Use of cefuroxime for women with community-onset acute pyelonephritis caused by cefuroxime-susceptible or -resistant Escherichia coli.* (2005-6648 (Electronic)).
98. Narchi, H. and M. Al-Hamdani, *Uropathogen resistance to antibiotic prophylaxis in urinary tract infections.* (1931-8448 (Electronic)).
99. Wagenlehner, F., et al., *Explorative Randomized Phase II Clinical Study of the Efficacy and Safety of Finafloxacin versus Ciprofloxacin for Treatment of Complicated Urinary Tract Infections. LID - 10.1128/AAC.02317-17 [doi] LID - e02317-17.* (1098-6596 (Electronic)).
100. Yao, J., et al., *Cefiderocol: An Overview of Its in-vitro and in-vivo Activity and Underlying Resistant Mechanisms.* (2296-858X (Print)).
101. Vahlensieck, W., et al., *Management of uncomplicated recurrent urinary tract infections.* 2016. **15**(4): p. 95-101.
102. Bronzwaer, S.L., et al., *A European study on the relationship between antimicrobial use and antimicrobial resistance.* (1080-6040 (Print)).
103. Ventola, C.L., *The antibiotic resistance crisis: part 2: management strategies and new agents.* (1052-1372 (Print)).
104. Goff, D.A., et al., *A global call from five countries to collaborate in antibiotic stewardship: united we succeed, divided we might fail.* (1474-4457 (Electronic)).
105. Fleming-Dutra, K.E., et al., *Prevalence of Inappropriate Antibiotic Prescriptions Among US Ambulatory Care Visits, 2010-2011.* (1538-3598 (Electronic)).
106. Landers, T.F., et al., *A review of antibiotic use in food animals: perspective, policy, and potential.* (1468-2877 (Electronic)).
107. Tümmler, B.A.-O., *Emerging therapies against infections with Pseudomonas aeruginosa. LID - F1000 Faculty Rev-1371 [pii] LID - 10.12688/f1000research.19509.1 [doi].* (2046-1402 (Electronic)).
108. Kennedy, D.A.-O.X. and A.A.-O. Read, *Why does drug resistance readily evolve but vaccine resistance does not? LID - 10.1098/rspb.2016.2562 [doi] LID - 20162562.* (1471-2954 (Electronic)).
109. Jansen, K.U., C. Knirsch, and A.S. Anderson, *The role of vaccines in preventing bacterial antimicrobial resistance.* (1546-170X (Electronic)).
110. Lipsitch, M. and G.R. Siber, *How Can Vaccines Contribute to Solving the Antimicrobial Resistance Problem? LID - 10.1128/mBio.00428-16 [doi] LID - e00428-16.* (2150-7511 (Electronic)).
111. Kwong, J.C., et al., *The effect of universal influenza immunization on antibiotic prescriptions: an ecological study.* (1537-6591 (Electronic)).

112. Cryz, S.J., Jr., et al., *Safety and immunogenicity of Escherichia coli O18 O-specific polysaccharide (O-PS)-toxin A and O-PS-cholera toxin conjugate vaccines in humans.* (0022-1899 (Print)).
113. Bien, J., O. Sokolova, and P. Bozko, *Role of Uropathogenic Escherichia coli Virulence Factors in Development of Urinary Tract Infection and Kidney Damage.* International Journal of Nephrology, 2012. **2012**: p. 681473.
114. Loubet, P., et al., *Alternative Therapeutic Options to Antibiotics for the Treatment of Urinary Tract Infections.* (1664-302X (Print)).
115. Tammen, H., *Immunobiotherapy with Uro-Vaxom in recurrent urinary tract infection. The German Urinary Tract Infection Study Group.* (0007-1331 (Print)).
116. Bauer, H.W., et al., *A long-term, multicenter, double-blind study of an Escherichia coli extract (OM-89) in female patients with recurrent urinary tract infections.* (0302-2838 (Print)).
117. Magasi, P., et al., *Uro-Vaxom and the management of recurrent urinary tract infection in adults: a randomized multicenter double-blind trial.* (0302-2838 (Print)).
118. Schulman, C.C., et al., *Oral immunotherapy of recurrent urinary tract infections: a double-blind placebo-controlled multicenter study.* (0022-5347 (Print)).
119. Brodie, A., et al., *A Retrospective Study of Immunotherapy Treatment with Uro-Vaxom (OM-89®) for Prophylaxis of Recurrent Urinary Tract Infections.* (1661-7649 (Print)).
120. Hopkins, W.J. and D.T. Uehling, *Vaccine Development for the Prevention of Urinary Tract Infections.* (1523-3847 (Print)).
121. Aziminia, N.A.-O., et al., *Vaccines for the prevention of recurrent urinary tract infections: a systematic review.* (1464-410X (Electronic)).
122. Ramírez Sevilla, C.A.-O., et al., *Active immunoprophyilaxis with uromune® decreases the recurrence of urinary tract infections at three and six months after treatment without relevant secondary effects.* (1471-2334 (Electronic)).
123. Nickel, J.C., P. Saz-Leal, and R.C. Doiron, *Could sublingual vaccination be a viable option for the prevention of recurrent urinary tract infection in Canada? A systematic review of the current literature and plans for the future.* (1911-6470 (Print)).
124. Huttner, A. and V. Gambillara, *The development and early clinical testing of the ExPEC4V conjugate vaccine against uropathogenic Escherichia coli.* (1469-0691 (Electronic)).
125. Cryz, S.J., Jr., et al., *Immunization of cystic fibrosis patients with a Pseudomonas aeruginosa O-polysaccharide-toxin A conjugate vaccine.* (0301-0457 (Print)).
126. Huttner, A., et al., *Safety, immunogenicity, and preliminary clinical efficacy of a vaccine against extraintestinal pathogenic Escherichia coli in women with a history of recurrent urinary tract infection: a randomised, single-blind, placebo-controlled phase 1b trial.* (1474-4457 (Electronic)).
127. Inoue, M., et al., *Safety, tolerability and immunogenicity of the ExPEC4V (JNJ-63871860) vaccine for prevention of invasive extraintestinal pathogenic Escherichia coli disease: A phase 1, randomized, double-blind, placebo-controlled study in healthy Japanese participants.* (2164-554X (Electronic)).
128. Frenck, R.W., Jr., et al., *Safety and immunogenicity of a vaccine for extra-intestinal pathogenic Escherichia coli (ESTELLA): a phase 2 randomised controlled trial.* (1474-4457 (Electronic)).
129. Guachalla, L.M., et al., *Multiple modes of action of a monoclonal antibody against multidrug-resistant Escherichia coli Sequence Type 131-H 30.* 2017. **61**(11): p. e01428-17.
130. Guachalla, L.M., et al., *Retained activity of an O25b-specific monoclonal antibody against an Mcr-1-producing Escherichia coli sequence type 131 strain.* 2018. **62**(7): p. e00046-18.
131. Henriques, P., et al., *Structure of a protective epitope reveals the importance of acetylation of Neisseria meningitidis serogroup A capsular polysaccharide.* 2020. **117**(47): p. 29795-29802.

132. Huesca, M., et al., *Synthetic peptide immunogens elicit polyclonal and monoclonal antibodies specific for linear epitopes in the D motifs of Staphylococcus aureus fibronectin-binding protein, which are composed of amino acids that are essential for fibronectin binding.* (0019-9567 (Print)).
133. Whittle, J.R., et al., *Broadly neutralizing human antibody that recognizes the receptor-binding pocket of influenza virus hemagglutinin.* (1091-6490 (Electronic)).
134. Burkhart, M.D., et al., *Distinct mechanisms of neutralization by monoclonal antibodies specific for sites in the N-terminal or C-terminal domain of murine leukemia virus SU.* (0022-538X (Print)).
135. Kisiela, D.I., et al., *Inhibition and Reversal of Microbial Attachment by an Antibody with Parasteric Activity against the FimH Adhesin of Uropathogenic E. coli.* (1553-7374 (Electronic)).
136. Kisiela, D.I., et al., *Conformational inactivation induces immunogenicity of the receptor-binding pocket of a bacterial adhesin.* Proceedings of the National Academy of Sciences, 2013. **110**(47): p. 19089-19094.
137. Jones, C.H., et al., *FimH adhesin of type 1 pili is assembled into a fibrillar tip structure in the Enterobacteriaceae.* 1995. **92**(6): p. 2081-2085.
138. Hahn, E., et al., *Exploring the 3D molecular architecture of Escherichia coli type 1 pili.* 2002. **323**(5): p. 845-857.
139. Spaulding, C.N., et al., *Functional role of the type 1 pilus rod structure in mediating host-pathogen interactions.* eLife, 2018. **7**: p. e31662.
140. Wright, K.J., S.J. Seed Pc Fau - Hultgren, and S.J. Hultgren, *Uropathogenic Escherichia coli flagella aid in efficient urinary tract colonization.* (0019-9567 (Print)).
141. Wurpel, D.J., et al., *Chaperone-usher fimbriae of Escherichia coli.* (1932-6203 (Electronic)).
142. Schwan, W.R., *Regulation of fim genes in uropathogenic Escherichia coli.* (2220-3176 (Print)).
143. Waksman, G. and S.J.J.N.R.M. Hultgren, *Structural biology of the chaperone–usher pathway of pilus biogenesis.* 2009. **7**(11): p. 765-774.
144. Abraham Jm Fau - Freitag, C.S., et al., *An invertible element of DNA controls phase variation of type 1 fimbriae of Escherichia coli.* (0027-8424 (Print)).
145. Klemm, P., *Two regulatory fim genes, fimB and fimE, control the phase variation of type 1 fimbriae in Escherichia coli.* (0261-4189 (Print)).
146. Kulasekara, H.D. and I.C. Blomfield, *The molecular basis for the specificity of fimE in the phase variation of type 1 fimbriae of Escherichia coli K-12.* (0950-382X (Print)).
147. Gally, D.L., I.C. Leathart J Fau - Blomfield, and I.C. Blomfield, *Interaction of FimB and FimE with the fim switch that controls the phase variation of type 1 fimbriae in Escherichia coli K-12.* (0950-382X (Print)).
148. Valenski, M.L., et al., *The Product of the fimI gene is necessary for Escherichia coli type 1 pilus biosynthesis.* (0021-9193 (Print)).
149. Klemm P Fau - Jørgensen, B.J., et al., *The fim genes responsible for synthesis of type 1 fimbriae in Escherichia coli, cloning and genetic organization.* (0026-8925 (Print)).
150. Jones, C.H., et al., *FimC is a periplasmic PapD-like chaperone that directs assembly of type 1 pili in bacteria.* (0027-8424 (Print)).
151. Freitag Cs Fau - Eisenstein, B.I. and B.I. Eisenstein, *Genetic mapping and transcriptional orientation of the fimD gene.* (0021-9193 (Print)).
152. Waksman, G. and S.J. Hultgren, *Structural biology of the chaperone–usher pathway of pilus biogenesis.* Nature Reviews Microbiology, 2009. **7**(11): p. 765-774.
153. Thomas, W.E., et al., *Bacterial adhesion to target cells enhanced by shear force.* 2002. **109**(7): p. 913-923.

154. Eto, D.S., et al., *Integrin-mediated host cell invasion by type 1-piliated uropathogenic Escherichia coli.* (1553-7374 (Electronic)).
155. Kline, K.A., et al., *Bacterial adhesins in host-microbe interactions.* (1934-6069 (Electronic)).
156. Sauer, M.M., et al., *Catch-bond mechanism of the bacterial adhesin FimH.* Nature Communications, 2016. **7**(1): p. 10738.
157. Magala, P., et al., *RMSD analysis of structures of the bacterial protein FimH identifies five conformations of its lectin domain.* (1097-0134 (Electronic)).
158. Le Trong, I., et al., *Structural basis for mechanical force regulation of the adhesin FimH via finger trap-like β sheet twisting.* 2010. **141**(4): p. 645-655.
159. Han, Z., et al., *Structure-based drug design and optimization of mannoside bacterial FimH antagonists.* 2010. **53**(12): p. 4779-4792.
160. Wellens, A., et al., *The tyrosine gate as a potential entropic lever in the receptor-binding site of the bacterial adhesin FimH.* 2012. **51**(24): p. 4790-4799.
161. Bouckaert, J., et al., *Receptor binding studies disclose a novel class of high-affinity inhibitors of the Escherichia coli FimH adhesin.* 2005. **55**(2): p. 441-455.
162. Vanwetswinkel, S., et al., *Study of the structural and dynamic effects in the FimH adhesin upon α-d-heptyl mannose binding.* 2014. **57**(4): p. 1416-1427.
163. Choudhury, D., et al., *X-ray structure of the FimC-FimH chaperone-adhesin complex from uropathogenic Escherichia coli.* 1999. **285**(5430): p. 1061-1066.
164. Sauer, M.M., et al., *Catch-bond mechanism of the bacterial adhesin FimH.* (2041-1723 (Electronic)).
165. Yakovenko, O., et al., *FimH forms catch bonds that are enhanced by mechanical force due to allosteric regulation.* (0021-9258 (Print)).
166. Bouckaert, J., et al., *Receptor binding studies disclose a novel class of high-affinity inhibitors of the Escherichia coli FimH adhesin.* (0950-382X (Print)).
167. Scharenberg, M., et al., *Target Selectivity of FimH Antagonists.* (1520-4804 (Electronic)).
168. Meiland, R., et al., *Fimch antiserum inhibits the adherence of Escherichia coli to cells collected by voided urine specimens of diabetic women.* (0022-5347 (Print)).
169. Connell, I., et al., *Type 1 fimbrial expression enhances Escherichia coli virulence for the urinary tract.* (0027-8424 (Print)).
170. Micoli, F., et al., *The role of vaccines in combatting antimicrobial resistance.* Nature Reviews Microbiology, 2021. **19**(5): p. 287-302.
171. Hanley, K.A., *The double-edged sword: How evolution can make or break a live-attenuated virus vaccine.* (1936-6426 (Print)).
172. Lopez-Sagaseta, J., et al., *Self-assembling protein nanoparticles in the design of vaccines.* Comput Struct Biotechnol J, 2016. **14**: p. 58-68.
173. Plotkin, S.J.P.o.t.N.A.o.S., *History of vaccination.* 2014. **111**(34): p. 12283-12287.
174. Wright Ae Fau - Semple, D. and D. Semple, *Remarks on Vaccination against Typhoid Fever.* (0007-1447 (Print)).
175. Parish, H.J.J.A.H.o.I., *A history of immunization.* 1965.
176. Holmgren, J., et al., *An oral B subunit-whole cell vaccine against cholera: from concept to successful field trial.* (0065-2598 (Print)).
177. Madsen, T.J.J.o.t.A.M.A., *Vaccination against whooping cough.* 1933. **101**(3): p. 187-188.
178. Thomas Jr, F., T.J.P.o.t.S.f.E.B. Magill, and Medicine, *Vaccination of human subjects with virus of human influenza.* 1936. **33**(4): p. 604-606.
179. Petrovsky, N. and J.C. Aguilar, *Vaccine adjuvants: current state and future trends.* (0818-9641 (Print)).
180. López-Sagaseta, J., et al., *Self-assembling protein nanoparticles in the design of vaccines.* Computational and structural biotechnology journal, 2015. **14**: p. 58-68.

181. Nguyen, B. and N.H. Tolia, *Protein-based antigen presentation platforms for nanoparticle vaccines.* NPJ Vaccines, 2021. **6**(1): p. 70.
182. Ljubojević, S., *The human papillomavirus vaccines.* (1330-027X (Print)).
183. Keating, G.M. and S. Noble, *Recombinant hepatitis B vaccine (Engerix-B): a review of its immunogenicity and protective efficacy against hepatitis B.* (0012-6667 (Print)).
184. Zhang, X., et al., *Robust manufacturing and comprehensive characterization of recombinant hepatitis E virus-like particles in Hecolin(®).* (1873-2518 (Electronic)).
185. Joyce, M.G., et al., *Efficacy of a Broadly Neutralizing SARS-CoV-2 Ferritin Nanoparticle Vaccine in Nonhuman Primates.* bioRxiv, 2021.
186. Aston-Deaville, S., et al., *An assessment of the use of Hepatitis B Virus core protein virus-like particles to display heterologous antigens from Neisseria meningitidis.* Vaccine, 2020. **38**(16): p. 3201-3209.
187. Heppner, D.G., et al., *Towards an RTS,S-based, multi-stage, multi-antigen vaccine against falciparum malaria: progress at the Walter Reed Army Institute of Research.* Vaccine, 2005. **23**(17): p. 2243-2250.
188. Kaba, S.A., et al., *Self-assembling protein nanoparticles with built-in flagellin domains increases protective efficacy of a Plasmodium falciparum based vaccine.* Vaccine, 2018. **36**(6): p. 906-914.
189. Govasli, M.L., Y. Diaz, and P. Puntervoll, *Virus-like particle-display of the enterotoxigenic Escherichia coli heat-stable toxoid STh-A14T elicits neutralizing antibodies in mice.* (1873-2518 (Electronic)).
190. King, N.P. and Y.-T.J.C.o.i.s.b. Lai, *Practical approaches to designing novel protein assemblies.* 2013. **23**(4): p. 632-638.
191. Olshefsky, A., et al., *Engineering Self-Assembling Protein Nanoparticles for Therapeutic Delivery.* Bioconjugate Chemistry, 2022.
192. Rome, L.H. and V.A.J.A.N. Kickhoefer, *Development of the vault particle as a platform technology.* 2013. **7**(2): p. 889-902.
193. Yeates, T.O., Y. Liu, and J. Laniado, *The design of symmetric protein nanomaterials comes of age in theory and practice.* (1879-033X (Electronic)).
194. Van de Steen, A., et al., *Bioengineering bacterial encapsulin nanocompartments as targeted drug delivery system.* (2405-805X (Electronic)).
195. Azuma, Y., D. Edwardson Tgw Fau - Hilvert, and D. Hilvert, *Tailoring lumazine synthase assemblies for bionanotechnology.* (1460-4744 (Electronic)).
196. Khmelinskaia, A., A. Wargacki, and N.P. King, *Structure-based design of novel polyhedral protein nanomaterials.* (1879-0364 (Electronic)).
197. Ballister, E.R., et al., *In vitro self-assembly of tailorable nanotubes from a simple protein building block.* (1091-6490 (Electronic)).
198. Padilla, J.E., T.O. Colovos C Fau - Yeates, and T.O. Yeates, *Nanohedra: using symmetry to design self assembling protein cages, layers, crystals, and filaments.* (0027-8424 (Print)).
199. King, N.P., et al., *Computational design of self-assembling protein nanomaterials with atomic level accuracy.* (1095-9203 (Electronic)).
200. Anishchenko, I.A.-O., et al., *De novo protein design by deep network hallucination.* (1476-4687 (Electronic)).
201. Sornay, C., et al., *An overview of chemo- and site-selectivity aspects in the chemical conjugation of proteins.* Royal Society Open Science. **9**(1): p. 211563.
202. Berti, F. and R. Adamo, *Antimicrobial glycoconjugate vaccines: an overview of classic and modern approaches for protein modification.* Chemical Society Reviews, 2018. **47**(24): p. 9015-9025.
203. Diaz, D., A.A.-O. Care, and A.A.-O. Sunna, *Bioengineering Strategies for Protein-Based Nanoparticles. LID - 10.3390/genes9070370 [doi] LID - 370.* (2073-4425 (Print)).

204. Veggiani, G., B. Zakeri, and M. Howarth, *Superglue from bacteria: unbreakable bridges for protein nanotechnology.* (1879-3096 (Electronic)).
205. Brune, K.D., et al., *Plug-and-Display: decoration of Virus-Like Particles via isopeptide bonds for modular immunization.* (2045-2322 (Electronic)).
206. Aranko, A.S., A. Wlodawer, and H. Iwaï, *Nature's recipe for splitting inteins.* (1741-0134 (Electronic)).
207. Pishesha, N., J.R. Ingram, and H.L. Ploegh, *Sortase A: A Model for Transpeptidation and Its Biological Applications.* (1530-8995 (Electronic)).
208. Patterson, D., et al., *Sortase-mediated ligation as a modular approach for the covalent attachment of proteins to the exterior of the bacteriophage P22 virus-like particle.* 2017. **28**(8): p. 2114-2124.
209. Guex, N. and M.C. Peitsch, *SWISS-MODEL and the Swiss-PdbViewer: an environment for comparative protein modeling.* (0173-0835 (Print)).
210. Song, Y., et al., *High-resolution comparative modeling with RosettaCM.* Structure (London, England : 1993), 2013. **21**(10): p. 1735-1742.
211. Thompson, J. and D. Baker, *Incorporation of evolutionary information into Rosetta comparative modeling.* Proteins, 2011. **79**(8): p. 2380-8.
212. Bradley, P., K.M. Misura, and D. Baker, *Toward high-resolution de novo structure prediction for small proteins.* Science, 2005. **309**(5742): p. 1868-71.
213. Schrodinger, LLC, *The PyMOL Molecular Graphics System, Version 1.8*. 2015.
214. Pettersen, E.F., et al., *UCSF ChimeraX: Structure visualization for researchers, educators, and developers.* Protein science : a publication of the Protein Society, 2021. **30**(1): p. 70-82.
215. Vetsch, M., P. Sebbel, and R. Glockshuber, *Chaperone-independent Folding of Type 1 Pilus Domains.* Journal of Molecular Biology, 2002. **322**(4): p. 827-840.
216. Tchesnokova, V., et al., *Type 1 fimbrial adhesin FimH elicits an immune response that enhances cell adhesion of Escherichia coli.* (1098-5522 (Electronic)).
217. Rabbani, S., et al., *Conformational switch of the bacterial adhesin FimH in the absence of the regulatory domain: Engineering a minimalistic allosteric system.* (1083-351X (Electronic)).
218. Phan, G., et al., *Crystal structure of the FimD usher bound to its cognate FimC-FimH substrate.* (1476-4687 (Electronic)).
219. Kisiela, D.I., et al., *Conformational inactivation induces immunogenicity of the receptor-binding pocket of a bacterial adhesin.* (1091-6490 (Electronic)).
220. Hsia Y Fau - Bale, J.B., et al., *Design of a hyperstable 60-subunit protein dodecahedron. [corrected].* (1476-4687 (Electronic)).
221. Bruun, T.U.J., et al., *Engineering a Rugged Nanoscaffold To Enhance Plug-and-Display Vaccination.* (1936-086X (Electronic)).
222. Zykova, A.A., et al., *Highly Immunogenic Nanoparticles Based on a Fusion Protein Comprising the M2e of Influenza A Virus and a Lipopeptide.* Viruses, 2020. **12**(10).
223. van Rosmalen, M., M. Krom, and M. Merkx, *Tuning the Flexibility of Glycine-Serine Linkers To Allow Rational Design of Multidomain Proteins.* Biochemistry, 2017. **56**(50): p. 6565-6574.
224. Song, Y., et al., *High-Resolution Comparative Modeling with RosettaCM.* Structure, 2013. **21**(10): p. 1735-1742.
225. Starks, C.A.-O., et al., *Optimization and qualification of an assay that demonstrates that a FimH vaccine induces functional antibody responses in women with histories of urinary tract infections.* (2164-554X (Electronic)).
226. Antonelli, G., et al., *Strategies to Tackle Antimicrobial Resistance: The Example of Escherichia coli and Pseudomonas aeruginosa. LID - 10.3390/ijms22094943 [doi] LID - 4943.* (1422-0067 (Electronic)).

227. Le Trong, I., et al., *Donor strand exchange and conformational changes during E. coli fimbrial formation.* (1095-8657 (Electronic)).